Contents lists available at ScienceDirect

Organic Geochemistry

journal homepage: www.elsevier.com/locate/orggeochem

Geochemistry of shale gases from around the world: Composition, origins, isotope reversals and rollovers, and implications for the exploration of shale plays

Alexei V. Milkov [a,*], Mohinudeen Faiz [b], Giuseppe Etiope [c,d]

[a] Colorado School of Mines, Golden, CO, USA
[b] CSIRO, Pullenvale, Queensland, Australia
[c] Istituto Nazionale di Geofisica e Vulcanologia, Rome, Italy
[d] Faculty of Environmental Science and Engineering, Babes-Bolyai University, Cluj-Napoca, Romania

ARTICLE INFO

ABSTRACT

We studied a large dataset of $\sim$2600 shale gas samples from 76 geological formations in 38 sedimentary basins located in eleven countries. Shale gases contain mostly hydrocarbons dominated by methane. Shale gases can have primary microbial, secondary microbial and thermogenic origin. However, gases produced from most commercially successful shale plays (e.g., the Marcellus, Haynesville, Eagle Ford and Barnett in the USA, the Vaca Muerta in Argentina and the Wufeng-Longmaxi in China) are thermogenic. It appears that formations with greater gas endowment such as the Marcellus and the Haynesville contain late-mature thermogenic gas. Shale plays with early-mature thermogenic and secondary microbial gas such as the Antrim (USA) and the New Albany (USA) formations have relatively low endowments of recoverable gas. Shale plays with primary microbial gas are not significant from commercial exploration perspective. Isotope reversals (δ^{13}C of methane > δ^{13}C of ethane) are observed in shale plays with mature organic matter (vitrinite reflectance > 2%) that experienced significant uplift (>2 km). It appears that isotope fractionation during desorption from depressurized late-mature shales leads to isotope reversal in the residual gas produced from shale formations (e.g., the Wufeng-Longmaxi). Significant contribution of adsorbed gas (enriched in ^{13}C-rich C_{2+} hydrocarbons relative to the co-occurring free gas) in the production from some plays (e.g., the Fayetteville, USA) may result in isotope rollovers.

© 2020 Elsevier Ltd. All rights reserved.

1. Introduction

Shales play an important role in petroleum (gas and oil) systems. They serve as source rocks and seals for conventional petroleum accumulations, and as reservoirs in unconventional systems where fracturing is required to enable sustainable petroleum flow. Production of natural gas from shales dates back to at least 1821, when the first commercial gas well in the USA was completed in the Devonian Dunkirk Shale (Peebles, 1980), and the gas was used to illuminate the town of Fredonia, New York (Roen, 1993). Production of gas from naturally fractured shales grew in the Appalachian Basin in the 19th and early 20th century (Curtis, 2002), but then was rapidly surpassed by production from conventional (sandstones and carbonates with relatively high permeability) reservoirs. Commercial production of shale gas in the USA started to

increase in the late 1970s (Hill and Nelson, 2000), but the total volumes of produced gases at the end of the 20th century were still <2% of the total USA production (Curtis, 2002). This changed in the early 21st century when advanced hydraulic fracturing of long horizontal wells led to a rapid growth of shale gas production. Since 2010, >20% of annual gas production in the USA come from shales, and the contribution of shales to total gas production is constantly growing. In 2018, about 23.6 trillion cubic feet (TCF, 667 billion m^3) of natural gas was withdrawn from shale gas wells in the USA, which accounted for about 64% of total gas withdrawals in the country (Energy Information Administration, 2019). Around the world, significant gas volumes are now produced from shale formations in Canada, China and Argentina.

The amount of available geochemical data on gas and oil from shales exponentially increased along with the growing production of petroleum from shale reservoirs. Fig. 1 illustrates the growth of published data on molecular and/or isotopic composition from shale gas samples from around the world over time. While many

* Corresponding author.
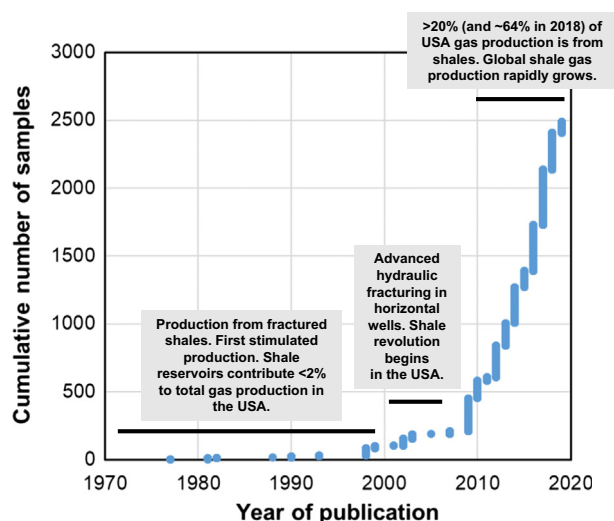 E-mail address: amilkov@mines.edu (A.V. Milkov).

Fig. 1. Exponential growth of published shale gas samples with molecular and/or isotopic compositions. The main developments in shale gas production through time are described.

authors discussed the composition and origin of gases from specific shale plays (e.g., Martini et al., 2003; Tilley et al., 2011; Zumberge et al., 2012; Liu et al., 2016a, 2016b), there are no recent studies on the origin of shale gas on the global scale.

Here, we study a global dataset of molecular and isotopic composition of shale gases from around the world. Our main objective is to interpret the origins of gases in shales and establish commonalities and differences between various shale plays. We will discuss isotope reversals and rollovers as these phenomena previously attracted special attention of many geochemists (Tilley and Muehlenbachs, 2013; Curiale and Curtis, 2016). Finally, we will discuss the implications of our findings for global exploration of shale gas resources.

2. Global dataset

The dataset includes molecular and isotopic composition of 2617 samples of gases from shale formations. This shale gas dataset is a subset of a larger global inventory of gas samples from conventional reservoirs, shales, coals, seeps and other geological habitats discussed by Milkov and Etiope (2018). However, the studied dataset includes additional 912 shale gas samples that became available to us since that publication. Gas data were collected from more than 110 peer-reviewed papers, government databases, research theses and reports. Most samples come from the USA (n = 1482), China (n = 567) and Canada (n = 367), and a smaller number of samples come from Sweden (n = 47), Argentina (n = 41), Saudi Arabia (n = 33), Australia (n = 30), Poland (n = 23), United Kingdom (n = 14), France (n = 9) and Russia (n = 4).

Most samples (n = 1847) are produced gases taken from wellheads or separators at the sites of shale gas production. There are also many gases desorbed at the surface from shale cores and cuttings (n = 575) and gases collected from the mudline during drilling through shale formations (n = 152). Most gases come from shales with established commercial gas production, such as Marcellus (e.g., Reese et al., 2014) and Barnett (Zumberge et al., 2012) formations in the USA. The produced gas may be free gas associated with relatively little condensate liquids (e.g., in the Haynesville Formation, Nicot et al., 2017) or oil-dissolved gas (e.g., in the Eagle Ford Formation, Byrne et al., 2018a, 2018b). There are also samples from shales that are not currently productive reservoirs (e.g., the Alum Formation in Sweden, Schovsbo and Nielsen, 2017).

The dataset includes samples from 38 sedimentary basins and 76 different formations (Fig. 2) ranging in age from Proterozoic (Kyalla and Velkerri formations, Australia, Faiz et al., 2018a, 2018b) to Miocene (e.g., Monterey and Antelope formations, USA, Lillis et al., 2007). Although most gas samples come from formations dominated by true shale lithology (e.g., the Marcellus Formation, USA), we, following Tilley and Muehlenbachs (2013), also include samples collected from unconventional "tight" plays where lithologies include very fine grained sandstone or siltstone (e.g., the Bakken Formation, USA) and some mixed clastic/carbonate reservoirs (e.g., the Niobrara Formation, USA and the Tuwaiq Formation, Saudi Arabia) where gases were generated within these formations or in immediately surrounding rocks. Formations with the largest number of gas samples in the dataset include Barnett (USA, n = 450) and Wufeng-Longmaxi (China, n = 319). The subsurface depth of shale gas samples varies from 2 m to 4600 m.

3. Results

The molecular and isotopic compositions of shale gases in the dataset vary widely (Table 1; Figs. 3–5). The composition of shale gases depends predominantly on the origin of gases, but can also be affected by the modality of gas occurrence (free gas, oil-dissolved gas, water-dissolved gas, adsorbed gas), the sampling technique, the degree of air contamination and other factors. Statistical data (especially the average values) reported below should be interpreted and used with caution because many gas samples have incomplete compositional data and the distribution of samples between different shale formations is highly uneven. The volume-weighted average shale gas composition discussed later in this paper better reflects the typical shale gas composition.

Another caveat is that gas measurements reported in published papers and reports used in this study may be not fully representative of gases within shale formations. Conventional petroleum reservoirs contain oil-dissolved or free gas in pore space, and molecular and isotopic composition of gas produced from conventional wells do not vary significantly with time (although such time-lapse gas studies are not common). Unconventional gas systems are more complex. For example, hydrate-bearing reservoirs may have varying molecular gas composition due to gas fractionation during gas hydrate formation (Sassen et al., 2000; Milkov et al., 2004). Both molecular and isotopic composition of coalbed gases may change during production (Mastalerz et al., 2017; Niemann and Whiticar, 2017) due to desorption, mixing and diffusion. Shales contain both free gas and gas adsorbed on the surface of clay minerals and organic matter. This introduces a potentially significant variability in gases partially extracted from the shale interval. Molecular and isotopic compositions of gases produced from shale formations may change over time (Sharma et al., 2015; Norville and Muehlenbachs, 2018; Zhang et al., 2018), presumably due to changing proportions of free and desorbed gases in the withdrawn gas. Gases liberated from shale cores and cuttings during degassing and desorption experiments at the surface have progressively different compositions (e.g., Ma et al., 2020) due to molecular and isotopic fractionation. In conventional systems, mud gases collected during drilling through petroleum-bearing reservoirs have many characteristics (such as ratio $CH_4/(C_2H_6 + C_3H_8)$ and $\delta^{13}C$-CH_4) largely similar to gases later produced from those reservoirs (Ellis et al., 2007; Milkov et al., 2007; Petersen et al., 2019). However, in unconventional shale systems mud gases collected during drilling may differ from produced formation gases. These caveats must be considered in case- and location-specific studies of shale gas geochemistry. Still, they are less important for the purpose of this paper, which is to interpret the origins of shale gases on a global scale.
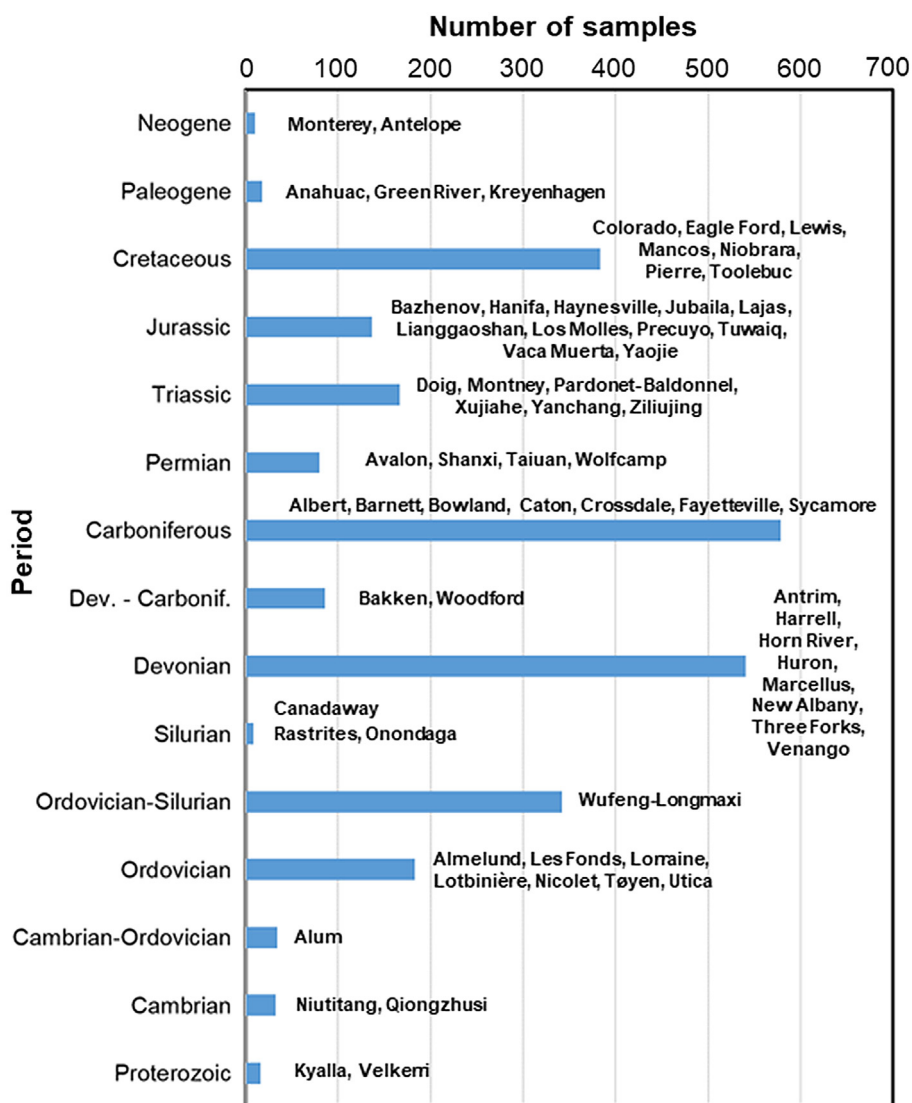
Fig. 2. Number of shale gas samples in the dataset coming from formations of different ages.

3.1. Molecular composition

Based on the measured gas composition, C_1–C_5 hydrocarbons (methane to pentanes) dominate in most shale gases (Fig. 3). Among hydrocarbons, methane (CH_4 or C_1) is the main component, followed by ethane (C_2H_6 or C_2) and propane (C_3H_8 or C_3). Methane is more abundant in produced shale gases (wellhead and separator samples) than in mud gases sampled during drilling and in gases released from shale cores and cuttings (Table 1). Gases released from shales during degassing experiments at the surface are, on average, significantly enriched in C_{2+} hydrocarbon gases relative to produced gases (Table 1).

Nitrogen (N_2) is an important non-hydrocarbon component in shale gas samples (Fig. 3). However, highly elevated N_2 often comes from sample treatment (e.g., Schulz et al., 2015) and from air contamination during sampling (e.g., Osborn and McIntosh, 2010; Reese et al., 2014). The average N_2 content in all available samples is 5.8 vol%, but the median N_2 content is only 1 vol% indicating that the average value is significantly affected by a relatively small number of samples with very high N_2 content (Fig. 3D). Shale gases from producing wells (from wellheads and separators) have average N_2 2.2 vol% (median 0.6%) (including some samples with air contamination). In contrast, desorbed gases often have elevated concentration of N_2, and its average is 22 vol% (median 11.8 vol%) (Table 1). It is possible that extra N_2 in cores and cuttings is derived through air contamination and oxidation while samples remain in desorption canisters over long periods (several weeks to months). However, the vast majority of these N_2-rich shale gases come from core desorption experiments in China (Liu et al., 2016a,b, 2018; Meng et al., 2017; Sun et al., 2017). These shale gases are significantly enriched in N_2 apparently by natural subsurface processes. For example, gases from the thermally over-mature Cambrian shale formations (Niutitang, Wangyinpu, Guanyintang) with complex tectonic history in the Yangtze platform (China) have 8–97 vol% of N_2, resulting presumably from thermal transformation of organic matter, ammonium in clay minerals, air from surface waters, and/or contribution from deep crust and mantle (Liu et al., 2016a; Wang et al., 2020).

Carbon dioxide (CO_2) is present in most shale gases. Its concentration averages 2.4 vol% (median 1.3 vol%) in all samples in the dataset (Fig. 3) and 2.1 vol% (median 1.3 vol%) in producing wells (Table 1). Elevated CO_2 concentrations are present in shales where oil biodegradation and secondary methanogenesis apparently occur, e.g., in the Monterey Formation, USA (Lillis et al., 2007)

Table 1
Mean (average) and median values for molecular and isotopic composition (selected characteristics) for shale gases sampled during production, drilling and degassing at the surface. NA – not available.

	Type of shale gases		
	Produced gases	Mud gas	Released from core or cuttings
		Where sampled	
	Wellhead or separator	Formation (during drilling)	Formation (at the surface)
	Concentration of methane (%)		
n of samples	1548	44	411
Mean	87.1	82.4	71.8
Median	91.0	77.1	77.0
	Concentration of C_{2+} gases (%)		
n of samples	1304	44	425
Mean	7.5	13.4	14.5
Median	2.3	8.9	8.3
	Concentration of nitrogen (%)		
n of samples	809	1	187
Mean	2.2	NA	22.0
Median	0.6	NA	11.8
	Concentration of CO_2 (%)		
n of samples	1210	27	211
Mean	2.1	3.3	4.4
Median	1.3	1.7	1.6
	$\delta^{13}C$ of methane (‰)		
n of samples	1656	149	526
Mean	−41.1	−40.8	−44.0
Median	−41.1	−43.9	−44.7
	$\delta^{13}C$ of ethane (‰)		
n of samples	1227	144	440
Mean	−36.0	−31.7	−35.8
Median	−35.2	−34.3	−34.8
	$\delta^{13}C$ of propane (‰)		
n of samples	937	144	339
Mean	−33.1	−28.7	−31.9
Median	−33.2	−30.7	−31.5

and in the Antrim Formation, USA (Wen et al., 2015). Other processes that may lead to elevated CO_2 in shale gases include thermochemical sulfate reduction (TSR) (e.g., the Pardonett-Baldonell play, Canada; Tilley et al., 2011) and supply of CO_2 from deep magmatic sources (e.g., the Vaca Muerta Formation, Argentina; Györe et al., 2017).

Hydrogen sulfide (H_2S) is not common in shales. However, H_2S is present in very high concentrations (up to 29.5 vol%) in the Pardonet-Baldonell play where it is a product of TSR reactions in shales interbedded with anhydrites (Tilley et al., 2011).

Helium (He) is present in shale gases in relatively low concentrations. There are 509 available measurements of He, and the average concentration is about 0.02 vol% (median 0.012 vol%). Shale gases, on average, have considerably lower content of He than gases from conventional petroleum reservoirs and gases from coals (Fig. 4). It appears that He in conventional reservoirs does not derive from the source rocks (mostly shales) as the hydrocarbons. This is a key demonstration that methane and helium in reservoir rocks are genetically untied; accordingly, interpretative parameters like $CH_4/^3He$ (e.g., Dai et al., 2008) can be misleading when applied to assess gas origin and migration in conventional petroleum systems.

3.2. Isotopic composition

Fig. 5 summarizes isotopic composition of carbon in methane, ethane, propane and CO_2 and isotopic composition of hydrogen in methane for available shale gas samples. Values of $\delta^{13}C$ of C_1, C_2 and C_3 have semi-normal distributions. However, values of $\delta^{13}C$ of CO_2 have a bi-modal distribution, and the distribution of δ^2H of C_1 is generally skewed towards the more positive values. These features result mostly from the origins of shale gases as discussed below.

4. Discussion

4.1. Origins of shale gases

Petroleum geochemists interpret molecular and isotopic composition of natural gases to understand their origins (primary or secondary microbial, thermogenic, abiotic), source rocks organofacies (marine shales, coals etc.) and post-generation processes (mixing, biodegradation, TSR etc.). These interpretations are commonly based on empirical binary gas genetic diagrams. The most utilized gas genetic diagrams include the diagram of $\delta^{13}C$-C_1 versus $C_1/(C_2 + C_3)$ first presented by Bernard et al. (1976, 1977), $\delta^{13}C$-C_1 versus δ^2H-C_1 proposed by Schoell (1983) and Whiticar et al. (1986), and $\delta^{13}C$-C_1 versus $\delta^{13}C$-CO_2 proposed by Gutsalo and Plotnikov (1981). Recently, Milkov and Etiope (2018) revised these three genetic diagrams using a global gas dataset of >20,000 samples from a wide variety of geological habitats.

All available $C_1/(C_2 + C_3)$, $\delta^{13}C$-C_1, δ^2H-C_1 and $\delta^{13}C$-CO_2 data for shale gases are plotted on the revised gas genetic diagrams in Fig. 6. It appears that the vast majority of shale gases have thermogenic origin. The maturity of these thermogenic gases varies widely from early-mature to late-mature gases, but most gases appear to be mid-mature (oil-associated) and late-mature. While secondary microbial gases formed during petroleum biodegradation are abundant in some shales, there are few shale gases with pure primary microbial origin. Produced shale gases have a narrower range of $\delta^{13}C$-C_1 than gases produced from conventional and coal gas reservoirs (Fig. 7), further supporting predominantly pure thermogenic origin and lower importance of gases with other origins or gases affected by post-generation processes.

Fig. 8 displays gas genetic diagrams for some of the main producing shale plays in the USA (Barnett, Eagle Ford, Fayetteville, Haynesville, Marcellus and Woodford), China (Wufeng-Longmaxi)
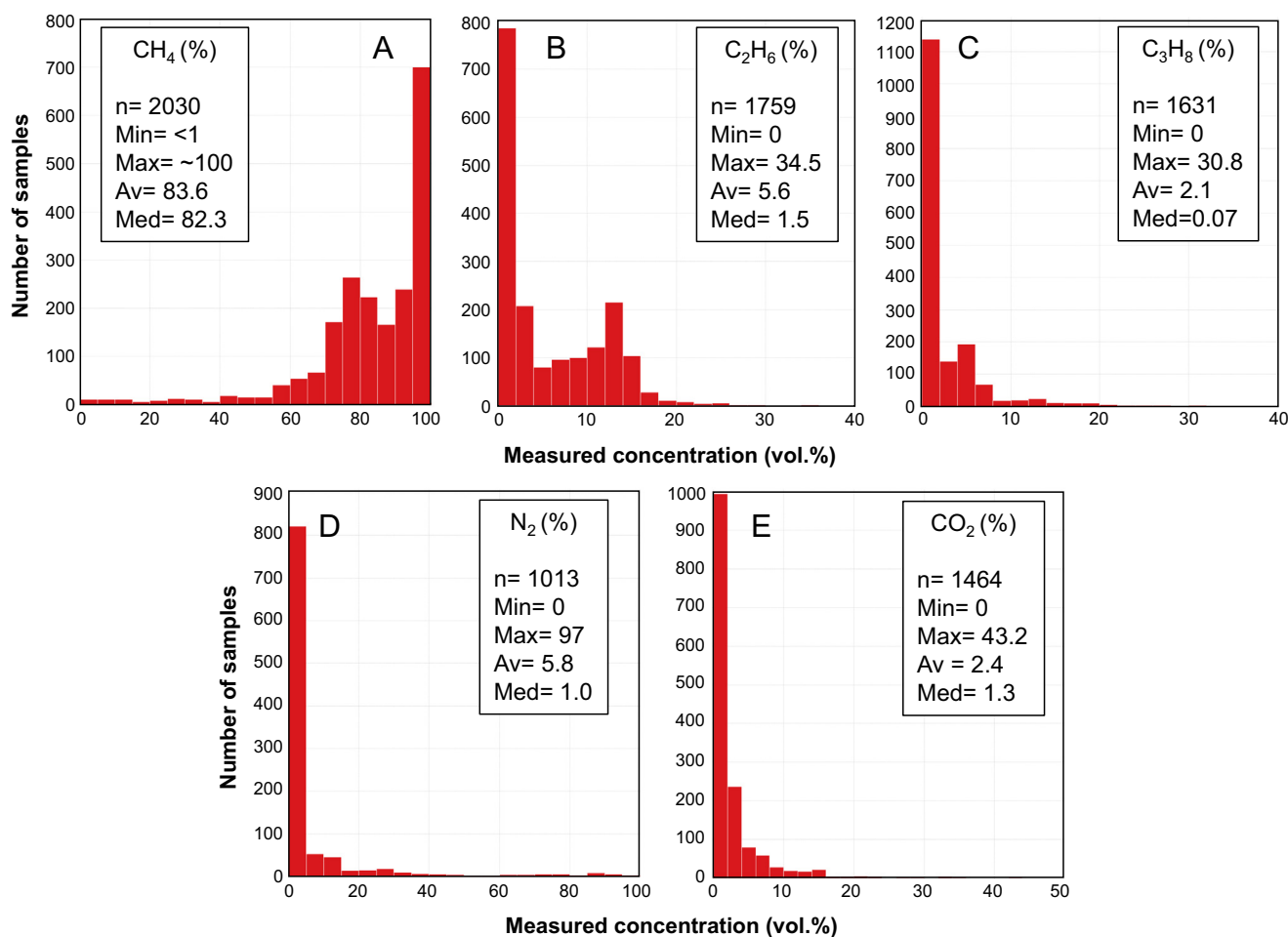
Fig. 3. Histograms showing measured concentrations (vol.%) of (A) methane (CH_4), (B) ethane (C_2H_6), (C) propane (C_3H_8), (D) nitrogen (N_2) and (E) carbon dioxide (CO_2) in shale gases from the studied dataset. Abbreviations: n – number of samples, Min – minimum, Max – maximum, Av – average (mean), Med- median.

and Argentina (Vaca Muerta). It is clear that gases from these most productive and commercially successful shale plays have pure thermogenic origin and vary in maturity from mid-mature (oil-associated) to late-mature gases.

Fig. 9 shows gas genetic diagrams for selected shale plays with secondary microbial gases. Such gases are especially prevalent in the Antrim Formation (Michigan Basin, USA) and the New Albany Formation (Illinois Basin, USA). Gases from the Antrim and the New Albany formations have often been considered as biogenic (primary microbial) or early-mature thermogenic (Dolton and Quinn, 1995; Martini et al., 2003; Nuttall, 2013). However, based on the revised genetic diagrams, we suggest that these gases are mixtures of early mature thermogenic gases and secondary microbial gases generated from biodegraded petroleum fluids. The main reason for such interpretation is that these gases have CO_2 highly enriched in ^{13}C, which is typical for secondary microbial gases (Milkov, 2011, 2018). The geological settings and evolutions of the Antrim Formation and the New Albany Formation are consistent with this interpretation of gas origin. Both shale formations experienced sufficient burial and thermal stress to generate oil (at least in some parts of the plays, East et al., 2012). During the uplift, they were brought to relatively shallow depth, where abundant fractures, low temperatures, and meteoric water from overlying aquifers (Formolo et al., 2008; Wen et al., 2015; Strąpoć et al., 2010) enabled microbial activity, oil biodegradation and secondary methanogenesis.

Fig. 10 displays gas genetic diagrams for shale plays with clear evidence of pure primary microbial gases in some samples from the Nicolet Formation (Canada) and the Alum Formation (Sweden). However, not all gases in these formations have primary microbial origin. Some gas samples have secondary microbial origin, early-mature thermogenic origin or are mixtures of primary microbial and early-mature thermogenic gases. The case of the Alum Formation demonstrates that shale gas can have different origins within one play, depending on the maturity and present-day burial depth of sample locations within the play (Schulz et al., 2015).

The concept of early-mature thermogenic gases is not new (e.g., Rowe and Muehlenbachs, 1999a,b; Coleman, 2001). However, gases recently sampled from several relatively low-mature shales provide clear evidence that early mature thermogenic gases indeed occur in the subsurface. They are drier (relatively more enriched in C_1) than oil-associated (mid-mature) thermogenic gases and have C_1 relatively enriched in [12]C ($\delta^{13}C$-C_1 as negative as −71‰). The main evidence that these gases have thermogenic origin comes from their semi-linear isotope profiles on the Chung's plot (Fig. 11, Chung et al., 1988). Such early-mature thermogenic gases are rarely found in conventional gas accumulations because they are not generated in large enough amounts to migrate and form separate accumulations. However, shale formations such as Colorado (Canada, Rowe and Muehlenbachs, 1999a,b), Green River (USA, Coleman, 2001), New Albany (USA, McIntosh et al., 2002) and Jurassic argillites in the Paris Basin (France, Prinzhofer et al.,
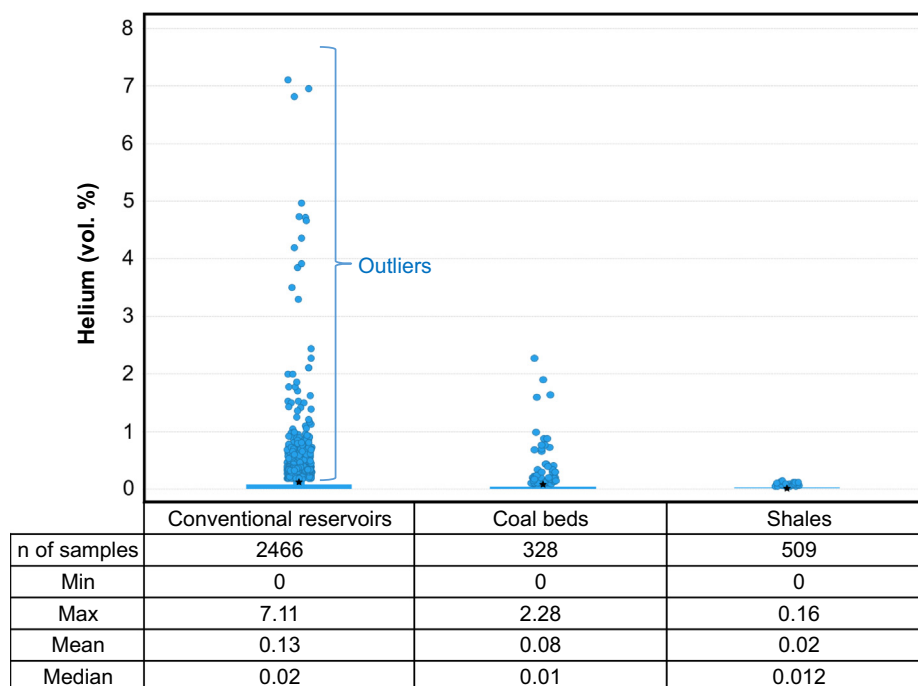
Fig. 4. Measured concentration of helium (He, vol.%) in gases from conventional reservoirs, coal beds and shales (the great majority of samples are produced gases sampled from wellheads). Data come from the global dataset of natural gases collected and described by Milkov and Etiope (2018), with additions. The data are displayed using box plots, which show average (mean) values as black stars, first quartile, third quartile, lower adjacent value, upper adjacent value, and outliers. The vast majority of values are located in the lower part of the distributions, and displayed statistical boundaries are poorly distinguished on these plots. They are better defined in Fig. 7 and the reader is encouraged to study that figure for the definitions of statistical parameters.

2009) do contain early-mature thermogenic gases, mostly formed *in situ* in relatively small amounts.

Mixing of natural gases is a common process in the subsurface (e.g., Milkov and Etiope, 2018). Gases in shales are usually regarded as generated *in situ* within the given shale formation with insignificant contribution of gases from other sources (other source rocks or non-sedimentary rocks and mantle). Although contribution from other sources is certainly possible in specific cases (e.g., Györe et al., 2017), our review of global geochemical data supports the idea that in general shales do not receive significant amounts of external gas. Fig. 6 shows that most shale gases generated through thermogenic processes and follow maturity trends very well, suggesting lack of significant mixing from different sources. Additional support for this comes from data on helium. Shale gases contain much less He than conventional reservoirs or coals (Fig. 4), and that He is of crustal and atmospheric origin (Fig. 12) (with an exception of some CO_2-enriched shale gases from the Vaca Muerta Formation, Argentina, where He apparently has mantle origin; Györe et al., 2017). Such relatively small concentration of He and its predominantly crustal/atmospheric origin suggest that shales are largely closed systems, where the lack of interaction with aquifers limits supply of external He (Byrne et al., 2018a, 2018b).

Still, gases within a given relatively small shale volume can originate from different processes. For example, many gases in the New Albany Formation are probably mixtures of early mature thermogenic gas and secondary microbial gas from biodegraded oil with a minor portion of primary microbial gas (Fig. 9). This complex gas origin reflects the geological history of the New Albany Formation with burial to oil window (East et al., 2012) around 280 Ma and subsequent uplift to present-day temperatures of 30–40 °C ideally suited for oil biodegradation (e.g., see Fig. 6 in Strąpoć et al., 2010).

4.2. Isotope reversals

Many papers discussing the geochemistry of shale gases address the observations and interpretations of isotope reversals (e.g., Zumberge et al., 2012; Tilley and Muehlenbachs, 2013; Dai et al., 2014; Xia et al., 2013; Cao et al., 2015; Faiz et al., 2018a, 2018b). However, most studies focus on individual shale plays or a selection of plays. In this section, we will discuss isotope reversals using our global dataset of shale gases as well as gases from other natural habitats.

Most individual natural gases have a "normal" carbon isotope trend for hydrocarbons, where $\delta^{13}C_1 < \delta^{13}C_2 < \delta^{13}C_3 < \delta^{13}C_{4n} < \delta^{13}C_{5n}$. This trend is typical for thermogenic gases and is consistent with the models of kinetic isotope effects (KIE) and laboratory gas generation experiments (e.g., Chung et al., 1988). Natural gases can also have isotope reversals, either partial (e.g., $\delta^{13}C_1 > \delta^{13}C_2 < \delta^{13}C_3$) or full ($\delta^{13}C_1 > \delta^{13}C_2 > \delta^{13}C_3$). Such gases have been found in abiotic systems (e.g., Sherwood Lollar et al., 2002), conventional petroleum reservoirs (e.g., Saadati et al., 2016; Shuai et al., 2018), fractured carbonate and tight sandstone reservoirs (e.g., Burrus and Laughrey, 2010) and desorbed coal gases (e.g., Faiz et al., 2018a, 2018b). The discussion and interpretation of isotope reversals intensified with the growing availability of shale gas data as many shale gases display such reversals. Fig. 13 demonstrates examples of normal isotope trend (also Fig. 11), full isotope reversal and various partial isotope reversals from shale plays around the world. Fig. 14 shows specific shale plays with and without isotope reversals.

Although some believe that isotope reversals are not commonly encountered in conventional petroleum reservoirs (e.g., Curiale and Curtis, 2016), data from the global gas dataset of Milkov and Etiope (2018) suggest that this is not the case. Fig. 15 shows that isotope reversals between methane and ethane ($\delta^{13}C$ of $C_1 > \delta^{13}C$

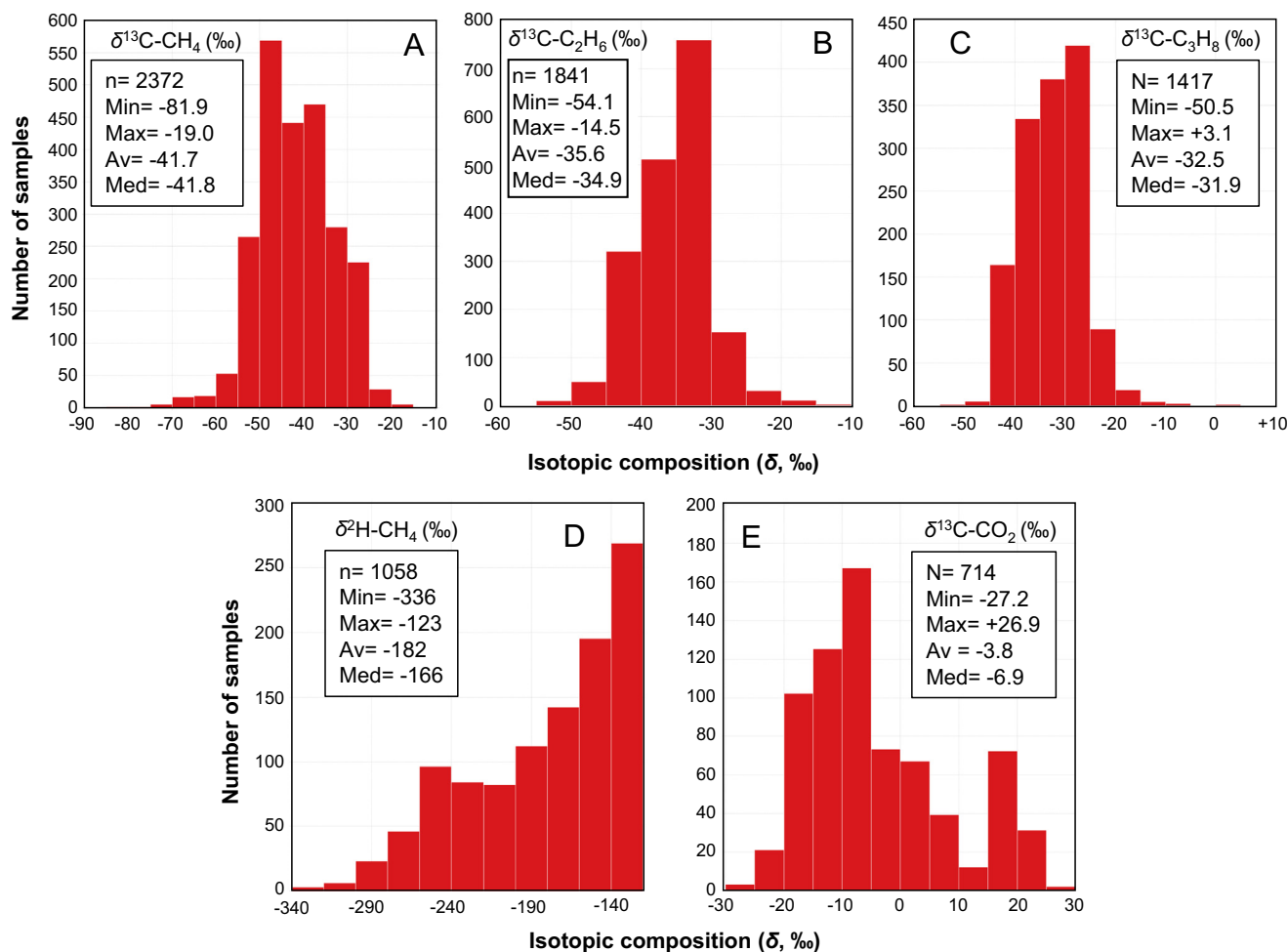**Fig. 5.** Histograms demonstrating the distribution of isotopic composition of gases from shales: (A) $\delta^{13}C$ of methane, (B) $\delta^{13}C$ of ethane, (C) $\delta^{13}C$ of propane, (D) δ^2H of methane, (E) $\delta^{13}C$ of carbon dioxide. Abbreviations as in Fig. 3.
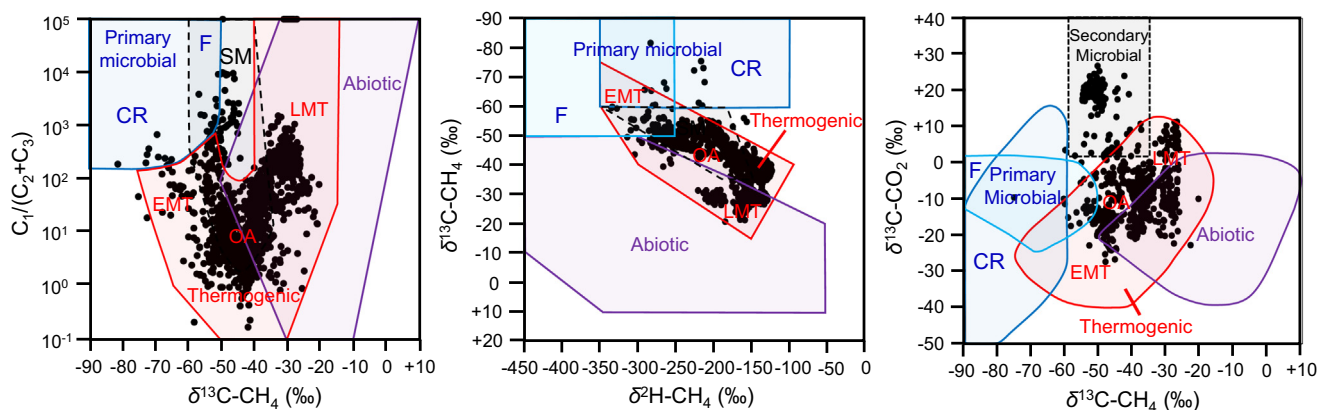

Fig. 6. Shale gases plotted on the revised gas genetic diagrams of Milkov and Etiope (2018). Abbreviations: CR – CO_2 reduction, F – methyl-type fermentation, SM – secondary microbial, EMT – early mature thermogenic gas, OA – oil-associated (mid-mature) thermogenic gas, LMT – late mature thermogenic gas.

of C_2) as well as ethane and propane ($\delta^{13}C$ of $C_2 > \delta^{13}C$ of C_3) are common both in conventional reservoirs and in shale formations. Reversed isotope trends appear to be mostly confined to mature gases with $\delta^{13}C$ of C_1 exceeding approximately −43‰ and dryness ratio $C_1/(\sum C_1$-$C_5)$ commonly exceeding 0.95 (Fig. 16).

There are shale plays where all currently available gas samples display isotope reversals, such as the Wufeng-Longmaxi Formation

(Liu et al., 2018) and the Velkerri Formation (Faiz et al., 2018a, 2018b). In other shale plays such as the Eagle Ford (Byrne et al., 2018a, 2018b) and the Haynesville Formation (Stolper et al., 2014; Byrne et al., 2020) all currently available samples have normal isotope trends. There are also shale plays where less mature areas have gases with normal isotope trends and more mature areas have gases with reversed isotope trends. This is the case,
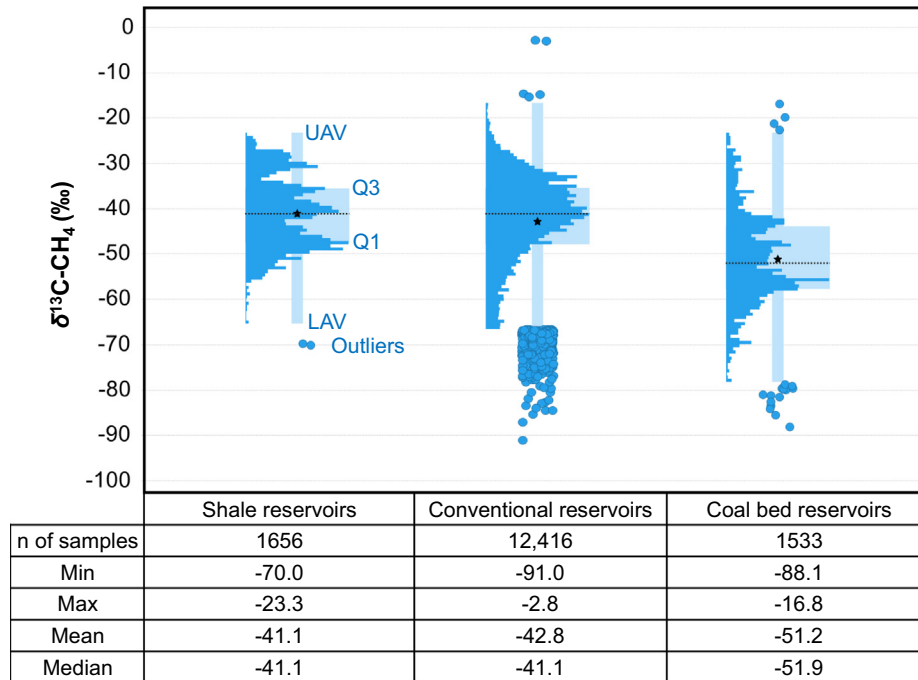
Fig. 7. Carbon isotopic composition of methane (δ^{13}C-CH$_4$) in produced gases from shale, conventional and coal bed reservoirs. Data come from the global dataset of natural gases collected and described by Milkov and Etiope (2018), with additions. The data are displayed using box plots, which show the distribution of data as histogram, average (mean) values as black star, median value as dotted black line, first quartile (Q1), third quartile (Q3), lower adjacent value (LAV), upper adjacent value (UAV), and outliers. The first quartile (Q1) is the median of the lower half of the data set. This means that about 25% of the values in the data set lie below Q1 and about 75% lie above Q1. The third quartile (Q3) is the median of the upper half of the data set. This means that about 75% of the values in the data set lie below Q3 and about 25% lie above Q3. The lower adjacent value is the smallest observation that is greater than or equal to the lower inner fence, which is the first quartile minus $1.5 \times$ IQR, where IQR stands for the interquartile range. The upper adjacent value is the largest observation that is less than or equal to the upper inner fence, which is the third quartile plus $1.5 \times$ IQR. Outliers are all values that fall outside of either of the fences.
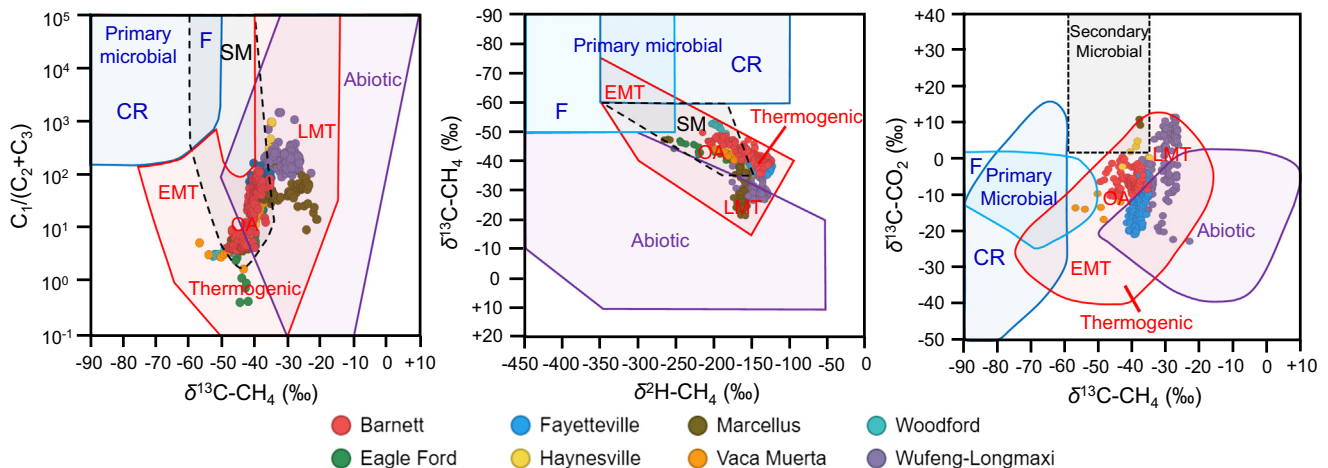

Fig. 8. Gases from some of the most productive shale plays plotted on the revised gas genetic diagrams of Milkov and Etiope (2018). Abbreviations are as in Fig. 8. The genetic field of thermogenic gases in the diagram of δ^{13}C-CH$_4$ vs δ^{13}C-CO$_2$ was slightly modified to include clearly thermogenic gases from the Marcellus formation.

for example, in the Marcellus Formation (Reese et al., 2014; Osborn and McIntosh, 2010) and in the Barnett Formation (Rodriquez and Philp, 2010).

Various hypotheses have been proposed to explain isotope reversals observed in shale gas reservoirs. Mixing of gases with different origins (for example, biotic and abiotic, Jenden et al., 1993) or from different source rocks (Dai et al., 2004) is one such hypothesis. Mixing of gasses generated from one shale formation at different stages of thermal maturity is also possible. For example, Xia et al. (2013) postulated that isotope reversal in low permeable shale reservoirs behaving as closed systems result from mixing of primary gases generated from cracking of kerogen and secondary gases generated through cracking of oil. They suggested that at maturities equivalent to R$_o$ > 2%, C$_1$ is largely produced through primary cracking of kerogen, while C$_2$ and C$_3$ come from secondary cracking of liquid petroleum. Although experimental evidence was not shown, they suggested that isotope fractionation during secondary cracking is stronger than during primary cracking and results in the production of isotopically light C$_2$ and C$_3$. Consequent mixing of gases from these two fractionation processes, within a low permeable over-pressured shales, leads to isotope reversal (Xia et al., 2013; Tilley et al., 2011).
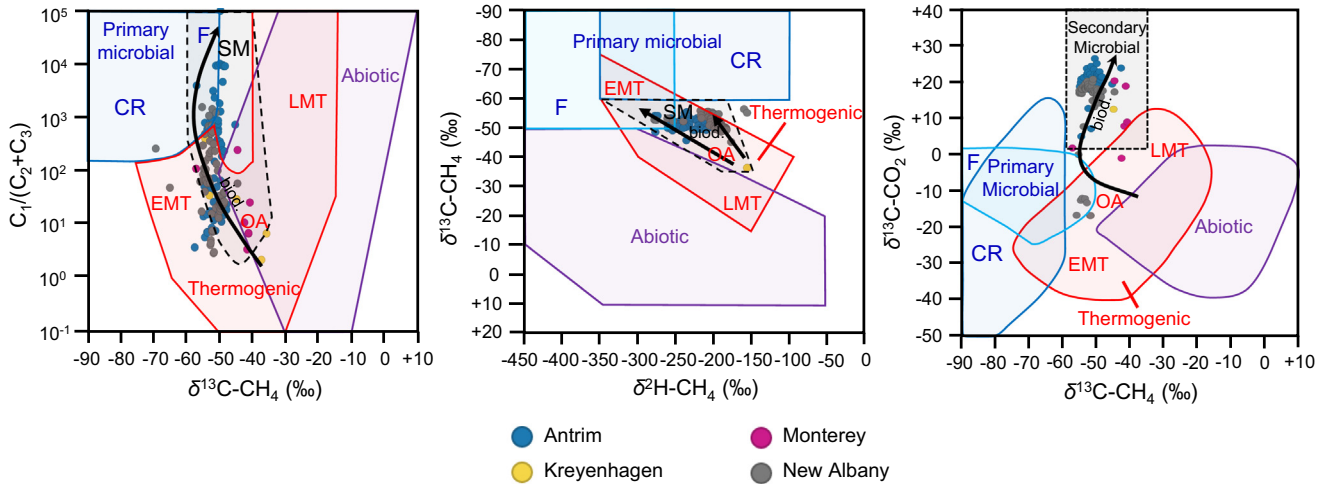
Fig. 9. Shale plays with secondary microbial gases plotted on the revised gas genetic diagrams of Milkov and Etiope (2018). Abbreviations are as in Fig. 8.
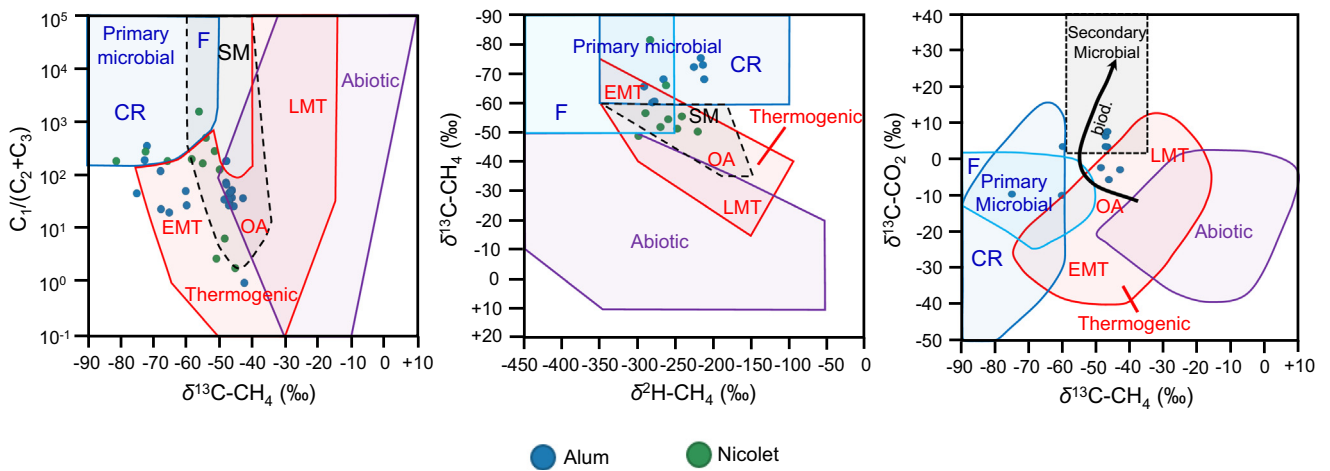

Fig. 10. Shale plays with primary microbial gases plotted on the revised gas genetic diagrams of Milkov and Etiope (2018). Abbreviations are as in Fig. 8.
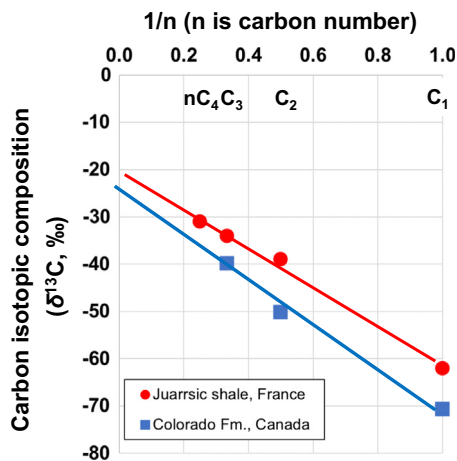

Fig. 11. Early mature thermogenic shale gases from the Jurassic shale in France (Prinzhofer et al., 2009) and the Colorado Formation in Canada (Rowe and Muehlenbachs, 1999a,b) displayed on the Chung plot (Chung et al., 1988).

Fig. 12. Concentration of helium (vol.%) and its isotopic composition (expressed as R/R_a) in conventional reservoirs, coals and shales. Data come from the global dataset of natural gases collected and described by Milkov and Etiope (2018), with additions.

Other hypotheses explaining isotope reversal and potentially relevant for shale reservoirs (Laughrey, 2014) include Rayleigh-type fractionation (Burruss and L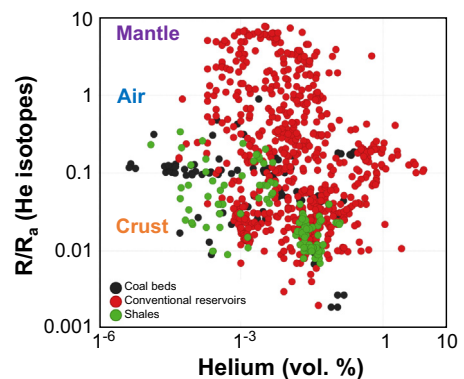aughrey, 2010; Pan et al., 2006), water-kerogen redox reactions (Burruss and Laughrey, 2010; Lewan, 1997; Price, 2001), carbon exchange at high temperature (Vinogradov and Galimov, 1970; Dai et al., 2016; Yang et al., 2017), water-reforming followed by Fischer-Tropsch synthesis (Tang and Xia, 2011) and destruction of C_{2+} alkanes followed by
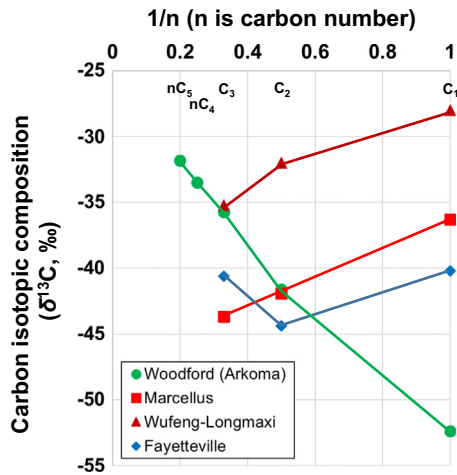
Fig. 13. Shale gases with normal and reverse isotope profiles displayed on the Chung plot (Chung et al., 1988). Sample from the Woodford Formation (Arkoma basin, USA, C. Liu et al., 2019) has normal isotope trend in which values of $\delta^{13}C$ increase (become less negative) as the carbon number of gases increase from methane (C_1) to n-pentane (n-C_5). Samples from the Marcellus Formation (Appalachian basin, USA, Reese et al., 2014) and the Wufeng-Longmaxi Formation (Sichuan basin, China, Feng et al., 2017) show complete isotope reversal trends where values of $\delta^{13}C$ become less negative as the carbon numbers of hydrocarbons increase. Sample from the Fayetteville Formation (Arkoma basin, USA, Zumberge et al., 2012) has a partial isotope reversal.

reforming via gas-phase radical recombination reactions (Telling et al., 2013). Isotope reversal may also result from aerobic and anaerobic microbial oxidation of some alkane components (Dai et al., 2004; James and Burns, 1984) and TSR (Hao et al., 2008; Krouse et al., 1988), but these processes are probably not common in thermally mature shales.

Another hypothesis for isotope reversal in shale and coal gas reservoirs is based on differential rates of molecular and isotope fractionation due to variations in adsorption and diffusivity properties of molecules. Numerous laboratory desorption studies have demonstrated that C_1 is released from carbonaceous rocks at a significantly faster rate than C_2 and C_3, causing an enrichment of C_{2+} components in the residual gas (Xia and Tang, 2012; Qin et al., 2017; Faiz et al., 2018a, 2018b; C. Liu et al., 2019; Z. Liu et al.,

2019; Cao et al., 2019; Ma et al., 2020). These studies also showed that hydrocarbons enriched in ^{12}C are released from shales more readily than those enriched in ^{13}C. As desorption progresses, isotopic enrichment (i.e., $\delta^{13}C$ value becoming less negative) in C_1 accelerates in accordance with the Rayleigh fractionation phenomenon (Faiz et al., 2018a, 2018b; C. Liu et al., 2019; Z. Liu et al., 2019). Therefore, due to the higher mobility of C_1 and ^{12}C, the isotope trend of the remaining gas in the shale becomes reversed. Such reversed isotope trends can be established in shale reservoirs that have reached dry gas maturity through deep burial and have subsequently desorbed gas during extensive basin inversion and depressurization. For example, relatively dry shale gas in the Mesoproterozoic Velkerri Formation (Beetaloo basin, Australia) was generated during the Paleozoic time when the shale was buried to depths exceeding 4 km. Subsequently, a significant amount of gas was expelled during the post-Paleozoic uplift of the shale to the current depth of about 2 km (Hoffman, 2016; Faiz et al., 2018b). Gas currently reservoired in the Velkerri shale shows a strongly reversed isotope trend suggesting that isotope fractionation has occurred through preferential desorption of lower molecular hydrocarbons and ^{12}C during >20 MPa of depressurization associated with basin inversion (Faiz et al., 2018a, 2018b).

Fig. 17 shows that isotope reversals between methane and ethane ($\delta^{13}C$ of $C_1 > \delta^{13}C$ of C_2) in conventional reservoirs occurs almost exclusively in onshore geological settings and are not common in gases sampled offshore. While most onshore petroleum systems experienced uplift and depressurization, most offshore petroleum systems are characterized by continuous burial with no or little depressurization. This may support the critical role of depressurization in the formation of gases with isotope reversals in late-mature source rocks.

To test this hypothesis, we compiled the dataset of thermal maturity and the amount of uplift for shale plays with and without isotope reversal between methane and ethane (Table 2). It appears that shale gas from plays that have lower maturity (vitrinite reflectance or VR < 2%) and relatively less uplift (<2 km) show no isotope reversal (e.g., the Eagle Ford and the Woodford (Anadarko basin) formations). In contrast, gases from mature shales (VR > 2%) that experienced significant uplift (>2 km) have isotope reversal (e.g., the Fayetteville and the Wufeng-Longmaxi formations). Gases from the relatively mature but not greatly uplifted Haynesville Formation do not have isotope reversal (based on data available so far),

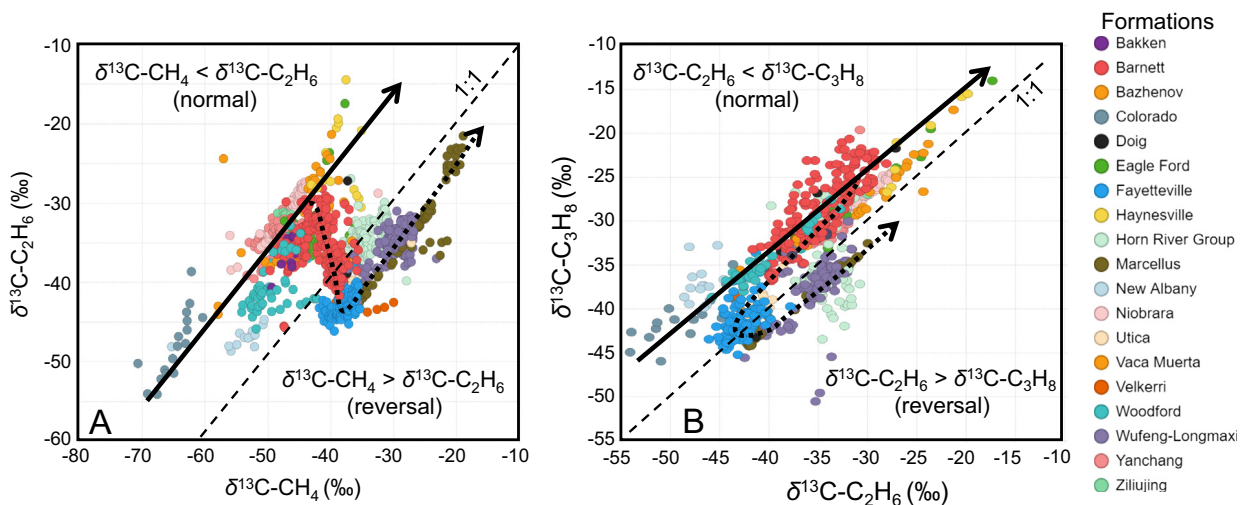**Fig. 14.** Carbon isotopic composition of methane and ethane (A) and ethane and propane (B) of thermogenic gases from selected shale formations. Solid black lines show the normal trend of increasing maturity. Dotted black lines show the increasing thermal maturity of gases with eventually full isotope reversal. Both plots show isotope reversals in most mature gases in the Marcellus and Wufeng-Longmaxi formations.
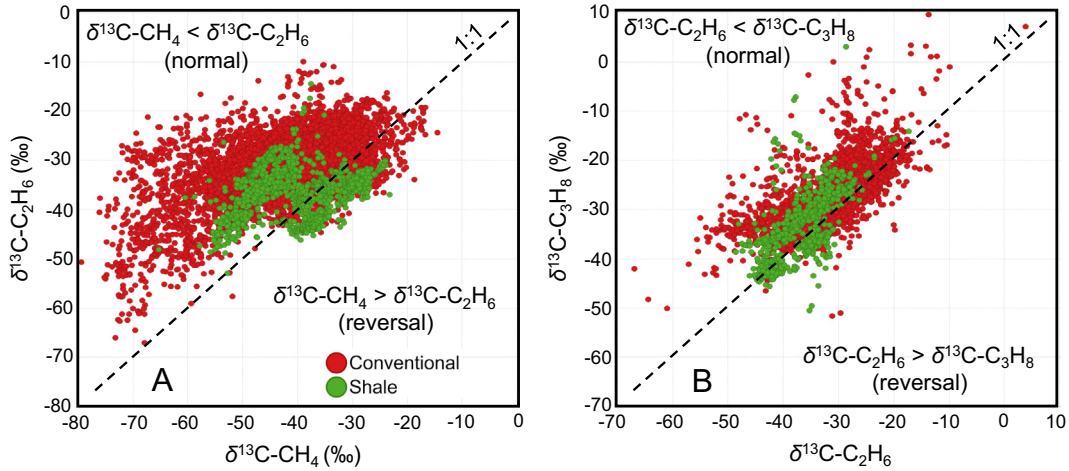
Fig. 15. Carbon isotopic composition of methane and ethane (A) and ethane and propane (B) of natural gases produced from conventional reservoirs and from shale (and some "tight") reservoirs.
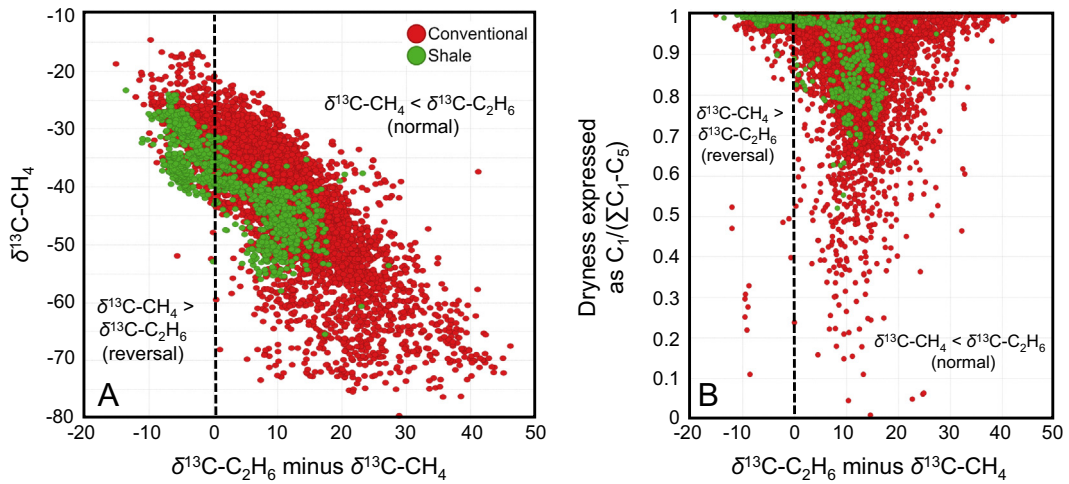

Fig. 16. Isotope reversal (expressed as a difference between $\delta^{13}C$ of ethane and $\delta^{13}C$ of methane) versus $\delta^{13}C$ of methane (A) and dryness of the gases (B) produced from conventional reservoirs and from shale (and some "tight") reservoirs. Dashed lines separate samples with reversal and samples without reversal.
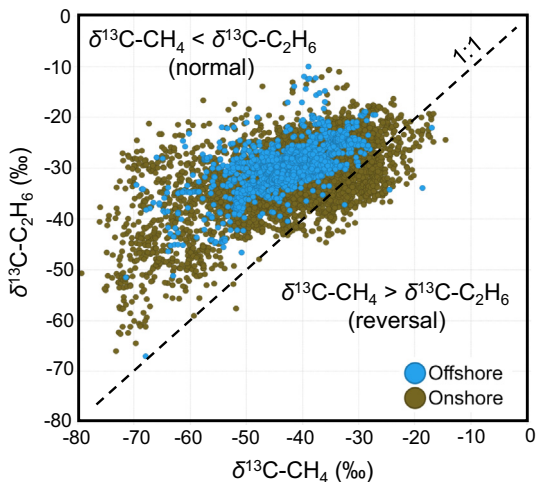

Fig. 17. Carbon isotopic composition of methane and ethane for natural gases sampled from onshore and offshore conventional reservoirs. Note that isotope reversal is not common in offshore samples.

which suggests that amount of uplift and related depressurization plays a more critical role in the creation of isotope reversal than thermal maturity. This is further supported by laboratory desorption experiments showing that later desorbed gases have isotope reversal even in relatively low mature (VR < 1%) rocks (e.g., Faiz et al., 2018b). As different parts of the play can have different maturity and uplift, gases with and without isotope reversals can occur in different parts of one play, as observed in the Marcellus and the Barnett formations. In the Barnett Formation, it appears that gases with isotope reversal occur in areas of greater thermal maturity and greater uplift (south and east), while there is no reversal in areas of less maturity and less uplift (north and west) (e.g., Rodriguez and Philp, 2010).

Our holistic geochemical and geological observations suggest that isotope reversals may be related to molecular and isotopic fractionation during differential desorption due to basin depressurization related to significant (>2 km) uplift of mature (VR > 2%) shale source rocks. The initial gas generated in the shale has normal isotope trend with $\delta^{13}C$ of $C_1 < \delta^{13}C$ of C_2. After the generation of the new gas essentially stops at high maturities (VR > 2%) and the uplift and depressurization begin, methane enriched in ^{12}C desorbs from the source rock more rapidly than methane enriched in ^{13}C. The residual methane becomes enriched in ^{13}C more rapidly

Table 2
Characteristics of shale plays with and without isotope reversal between $\delta^{13}C$ of methane and ethane. VR is vitrinite reflectance (or equivalent).

Formation name and type of gas	Approximate maturity, VR (%)	Average δ^{13}-CH_4 (‰, rounded)	Average δ^{13}-C_2H_6 (‰, rounded)	Amount of uplift (km, approximate)	References
Shale plays with no isotope reversal					
Colorado (formation gas)	0.25–0.4	−65	−48	0.45–1.5	Rowe and Muehlenbachs (1999a,b)
Bazhenov (formation gas)	0.6–0.7	−53	−42	0.5	Krasnova et al. (2019); uplift estimated from Ulmichek (2003) and Milkov (2010)
New Albany (formation gas)	0.52–0.68	−52	−43	1.5	Strąpoć et al. (2010)
New Albany (produced gas)	0.5–0.7	−53	−47	1.5	McIntosh et al. (2002), Nuttall et al. (2015), Salehi (2010), Schlegel et al. (2011); uplift estimated from Strąpoć et al. (2010)
Yanchang (formation gas)	1.2	−48	−34	1.5	Chen et al. (2016), Meng et al. (2017), Li et al. (2019); uplift estimated from Meng et al. (2017)
Yanchang (produced gas)	0.9–1.1	−49	−37	1.5	Dai et al. (2016), Chen et al. (2016); uplift estimated from Meng et al. (2017)
Eagle Ford (produced gas)	0.7–1.5	−43	−32	0.5–2	Byrne et al. (2018a), Clog et al. (2018), Douglas et al. (2017), He (2017), Piasecki et al. (2018); uplift estimated from Cander (2012)
Haynesville (produced gas)	1.7–2.5	−39	−25	0.3–1.2 (Late K) and 0–0.4 (recent)	Stolper et al. (2014), Nicot et al. (2017), Darling (2015), Byrne et al., (2020); uplift estimated from Williams (2013) and Nunn (2012)
Woodford, Anadarko basin (produced gas)	0.8–1.5	−49	−39	1.5	Zumberge et al. (2016), Kornacki and Dahl (2016), Abrams and Thomas (2020); uplift estimated from Cander (2012)
Shale plays with isotope reversal					
Velkerri (formation gas)	2.5	−34	−43	2.2 (Late Pz) and 1 (recent)	Faiz et al. (2018a, 2018b)
Velkerri (produced gas)	2.5	−38	−40	2.2 (Late Pz) and 1 (recent)	Faiz et al. (2018a, 2018b)
Fayetteville, Arkoma basin (produced gas)	2.5	−38	−43	>3	Zumberge et al. (2012); uplift estimated from Cander (2012) and Lamb (2014)
Wufeng-Longmaxi (produced gas)	2.5–3.3	−30	−35	3.5	Wei et al. (2016), Feng et al. (2017), Yang et al. (2017); Zhao et al. (2018); uplift estimated from Yang et al. (2017)
Shale plays with and without isotope reversal					
Marcellus (produced gas) with reversal (most Marcellus samples in the dataset)	2 to 4	−31	−38	3–5	Reese et al. (2014), Molofsky et al. (2013), Laughrey (2014); uplift estimated from Rowan (2006)
Marcellus (produced gas) without reversal	1–2	−43	−34	1–2	Osborn and McIntosh (2010), Jenden et al. (1993); uplift estimated from Rowan (2006)
Barnett (produced gas) with reversal	>1.65	−38	−39	2.1 (T-J) and 2 (recent)	Rodriguez and Philp (2010), Zumberge et al. (2012); uplift estimated from Jarvie (2004)
Barnett (produced gas) without reversal (most Barnett samples in the dataset)	<1.65	−43	−35	1.5 (T-J) and 1.5 (recent)	Rodriguez and Philp (2010), Zumberge et al. (2012), Nicot et al. (2017); uplift estimated from Jarvie (2004)

than residual ethane, which leads to isotope reversal of the residual gas in rocks that experienced significant uplift (>2 km) and depressurization (Faiz et al., 2018b). This residual gas with isotope reversal is produced, for example, from the Wufeng-Longmaxi Formation.

4.3. Isotope rollovers

It is generally accepted that as thermogenic gases become more mature, their wetness decreases (C_{2+} gases decrease, and dryness ratios such as $C_1/(C_2 + C_3)$ and $C_1/(\sum C_1$-$C_5)$ increase) while values of $\delta^{13}C$ of C_1-C_5 gases increase. This normal trend is observed within a group of gas from a single source, for example, within one petroleum system with a source rock of varying maturity. Isotope rollovers describe situations when this maturity trend "rolls over" and selected gas components become isotopically lighter (more negative values of $\delta^{13}C$) with increasing maturity (Curiale and Curtis, 2016). Classic examples of isotope rollover for ethane were presented by Zumberge et al. (2012) in the Barnett play (USA) and by Tilley and Muehlenbachs (2013) in the Montney-Doig play (Canada).

Fig. 18 shows the relationship between wetness (total C_{2+} gases) and $\delta^{13}C$ of C_1-C_3 in shale gases. There is no isotope rollover for methane. The maturity trend starts with the relatively dry gas (0.1–1 vol% C_{2+}) and methane enriched in ^{12}C ($\delta^{13}C_1$ around −70‰), although the data describing this low-maturity stage are still relatively sparse (Fig. 18A). As maturity increases, the gas becomes progressively enriched in C_{2+} and ^{13}C-C_1 (mid-mature or oil-associated gas), and then becomes depleted in C_{2+} but even more enriched in ^{13}C-C_1 at the late-mature stage. This is a normal isotope trend of maturity increase, and it also occurs in both onshore and offshore conventional reservoirs (Fig. 18D).

However, ethane and propane in many shale gases show isotope rollovers (Fig. 18B and C). While some shale gases become more enriched in ^{13}C-C_2 and ^{13}C-C_3 after the mid-mature stage (i. e, they follow normal trend of maturity increase), most gases in shale formations become depleted in ^{13}C-C_2 and ^{13}C-C_3 (e.g., the Barnett Formation) and have $\delta^{13}C$-C_2 values as low as −46‰ (e.g., the Fayetteville Formation) and $\delta^{13}C$-C_3 values as low as −50‰ (e.g., the Wufeng-Longmaxi Formations). Then, at the very late-mature stage when C_{2+} gases are < 1 vol%, ethane and propane become again enriched in ^{13}C (e.g., the Wufeng-Longmaxi Formation). That behavior of carbon isotopes of ethane and propane in shale gases is not normal. For example, the vast majority of thermogenic gases in conventional offshore accumulations follow the expected maturity trends and do not have rollovers for ethane and propane (Fig. 18E and F). This rollover trend is also not obvious in onshore conventional accumulations of thermogenic gas, but this may be because of mixing of gases from different source rocks with different maturities in relatively open petroleum systems.
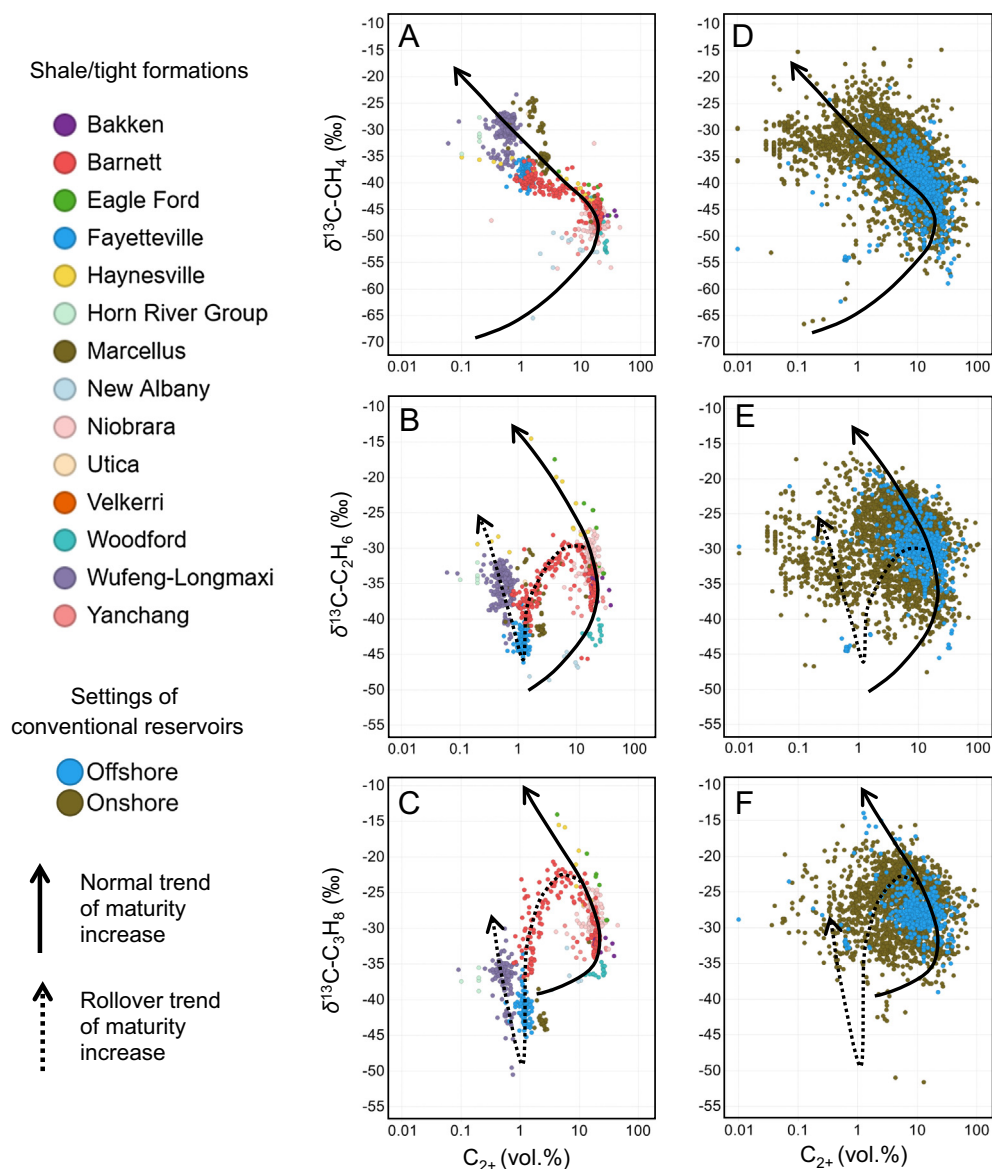
Fig. 18. Total volume of C_{2+} (ethane-pentane) hydrocarbons versus carbon isotopic composition ($\delta^{13}C$) of methane (A,D), ethane (B,E), and propane (C,F) in thermogenic gases produced from shale reservoirs (A–C) and from onshore and offshore conventional reservoirs (D–F).

Tilley and Muehlenbachs (2013) studied isotope rollovers in the North American sealed self-contained (shale) petroleum systems and demonstrated that rollover results from increasing thermal maturity. They also established that gases isotopically reversed with respect to methane and ethane occur in the latest stage of the rollover zone and in the post-rollover zone, which we confirm here. Still, they concluded that "the processes that cause the rollover are not well understood" (p. 204).

We observe that isotope reversals occur in both conventional (onshore, but not offshore) accumulations and in shale formations (Fig. 15). However, rollovers occur predominantly in shales (Fig. 18). Shale gases are residual gases left in source rocks after most of the generated gas (especially in late-mature shales) migrated into the overburden and conventional accumulations. This residual gas remains in free and adsorbed state in the shales before it is removed through production.

Wells in mid-mature shale formations with no isotope reversal produce mostly free gas, for example in the Eagle Ford Formation (about 80% free gas and 20% adsorbed gas) (De Silva et al., 2015; Li

et al., 2016). In contrast, wells in late-mature shale formations with isotope reversal produce a large portion of the adsorbed gas, for example, in the Fayetteville Formation (about 20% free gas and 80% adsorbed gas), Wufeng-Longmaxi Formation (about 60–80% of adsorbed gas, Cao et al., 2019) and in the Marcellus Formation (about 60% free gas and 40% adsorbed gas) (De Silva et al., 2015; Li et al., 2016). Experiments suggests that the amount of adsorbed methane is generally greater for shales that are richer in total organic carbon (TOC), are more thermally mature and have less moisture (Zhang et al., 2012). Within the same formation, the free gas is more enriched in methane (also relatively ^{12}C-rich) than in C_{2+} gases, while the adsorbed gas is more enriched in C_{2+} gases (also relatively ^{12}C-rich) and has methane significantly depleted in ^{12}C (Faiz et al., 2018a, 2018b). When produced, shales with dominant proportion of free gas have molecular and isotopic characteristics similar to conventional reservoirs and do not display rollovers in produced gases. However, shales with significant amount of adsorbed gas produce gas that is somewhat enriched in ^{12}C-rich C_{2+} gases relative to their maturity, resulting in isotope rollover.

It is possible to further test this hypothesis by studying molecular and isotopic composition of gases produced from the same shale well for a long time, but such time-lapse geochemical data are not common yet. Data for three wells each producing for 3.5 years from the Wufeng-Longmaxi formation indicate that gas becomes generally enriched in C_{2+} alkanes ($C_1/(C_2 + C_3)$ decreases) and its methane becomes more enriched in ^{13}C ($\delta^{13}C$-C_1 increases) as production progresses (Zhang et al., 2018). Norville and Muehlenbachs (2018) observed significant variations in $\delta^{13}C$-C_1 during about 3–4 years of production from shales of the Horn River Group, with a general enrichment in ^{13}C during production. These examples may suggest greater contribution of adsorbed (desorbed during production) gas with increasing production. In contrast, Sharma et al. (2015) presented data from two wells producing from the Marcellus Formation, in which $\delta^{13}C$-C_1 slightly but consistently decreased during 14 months following hydraulic fracturing. Although other geochemical processes can lead to isotope reversals and rollovers as reviewed above, it is possible that molecular and isotopic fractionation during desorption after depressurization – first, from the uplift and then from production – is the leading mechanism in shale plays.

4.4. Volume-weighted average shale gas composition and origin in the USA

Before discussing the molecular and isotopic composition of shale gases above, we cautioned that the statistical distributions and parameters like mean (average) values for the entire global dataset are not very meaningful. This is because the distribution of samples among shale formations is not even, e.g, we have 450 samples from the Barnett Formation (USA) and 319 samples from the Wufeng-Longmaxi Formation (China) but only one sample from each of the Amelund (Sweden), Canadaway (USA), Huron (USA), Phosphoria (USA), and Xujiahe (China) formations. In addition, the amount of shale gas stored in different plays varies widely as the result of shale gas origin, thermal maturity, rock volumes (area, thickness) and other factors. In this section, we attempt to overcome these problems and estimate the volume-weighted average composition and origin of shale gas in the USA. Such estimates may serve as useful inputs in various regional and global models involving natural gas composition, e.g., in models of methane emissions from shale gas developments to the atmosphere (Schwietzke et al., 2016; Howarth, 2019; Milkov et al., 2020). We included only shale plays from the USA in this exercise because

the gas endowment (production, reserves and resources) data from non-USA shale plays are less available, less certain and more controversial. For example, Potter (2018) reported the range of Paleozoic shale gas recoverable resources in the Sichuan Basin, China (largely in the Wufeng-Longmaxi Formation) from 93 to 626 tcf, and provided his own mean estimate of 23.9 tcf.

We estimated the volume-weighted average shale gas composition in the USA in two steps. First, we calculated the average molecular and isotopic composition for the main productive shale plays (Table 3). Then, we used the published estimates of gas endowment in those shale plays to weight the relative volumetric significance of each play (Table 3). The volume-weighted average shale gas in the USA is dominated by methane (89 vol%) and C_{2+} hydrocarbons (6.6 vol%) and has little non-hydrocarbon gases. This average gas has thermogenic origin and mid-to-late thermal maturity. This result is influenced by the volumetric dominance (60% of the total gas endowment) of relatively dry late-mature shale gas from the Marcellus Formation and the absence from the analysis of volumetrically significant shale plays with relatively wetter gas from the Permian Basin where little published gas data are available to date.

In the previous review of shale gases, Curtis (2002) studied five fractured shale plays in the USA and concluded that the shale gas has predominantly biogenic (microbial) origin. In contrast, our results based on a large number of gas samples recently collected from the largest and most productive shale plays clearly suggest that shale gases are predominantly thermogenic. Secondary microbial and primary microbial gases are volumetrically not significant in currently known commercially successful shale plays. This is similar to gases in global conventional petroleum accumulations, where thermogenic gases predominate ($\sim$85–92% of global gas endowment), followed by secondary microbial ($\sim$5–11%) and primary microbial ($\sim$3–4%) gases (Milkov, 2011).

4.5. Implications for exploration of shale plays

Shale gas exploration is driven, to a large extent, by the resource size of the shale plays, productivity of shale reservoirs (Initial Production (IP) and Expected Ultimate Recovery (EUR) of wells) and their commerciality. Our geochemical study of shale gases from around the world suggests that the best shale plays (i.e., those with largest resources and greatest productivity) contain gas of thermogenic origin. Examples include main shale plays in the USA such as Marcellus, Haynesville, Eagle Ford, and Barnett and commercially

Table 3

Gas endowment, play parameters and average gas composition for key shale plays in the USA. Gas endowment includes production to date, reserves (from Energy Information Administration, 2019) and resources of technically recoverable gas (from Potental Gas Agency, 2019). The approximate area of the plays was estimated from Energy Information Administration play map. Approximate average net thickness was estimated based on available play-specific publications and reports. Gas samples used for average gas composition calculations include mostly produced gases, but also some formation (desorbed gases and mud gases) gases. NA – not available.

| Shale Play	Gas endowment (volume), bcm/ tcf	Approximate area, km²	Approximate average net thickness, m	Normalized gas endowment, $10^3 \times m^3/km^2/m$	Number of gas samples	Average gas composition						
						C_1, %	C_{2+}, %	N_2, %	CO_2, %	$C_1/$ $(C_2 + C_3)$	$\delta^{13}C$ of C_1, ‰	δ^2H of C_1, ‰
Marcellus	28,487/1006	220,000	46	2815	106	93.0	2.8	3.4	0.0	51	−32.4	−166
Haynesville	5343/189	28,000	40	4771	34	88.9	7.2	2.2	2.2	238	−38.8	−155
Eagle Ford	4058/143	50,000	70	1159	95	66.3	23.6	0.2	1.4	5	−42.9	−202
Barnett	3775/133	70,000	90	599	450	88.8	9.3	1.0	1.5	32	−42.7	−153
Fayetteville	2396/85	15,000	41	3895	101	96.9	1.2	0.0	2.0	85	−38.2	−133
Woodford (Anadarko)	2036/72	17,000	49	2444	49	75.2	20.9	2.5	0.7	5	−49.0	NA
Woodford (Arkoma)	813/29	8,000	50	2032	18	77.1	22.0	NA	0.9	4	−49.4	−183
Antrim	279/10	109,000	30	85	114	83.9	2.9	7.8	6.4	2254	−51.3	−240
New Albany	103/4	32,000	23	140	122	88.0	2.4	2.6	3.9	218	−52.3	−202
Volume-weighted average gas composition						**89.0**	**6.6**	**2.5**	**0.7**	**79**	**−36.3**	**−167**
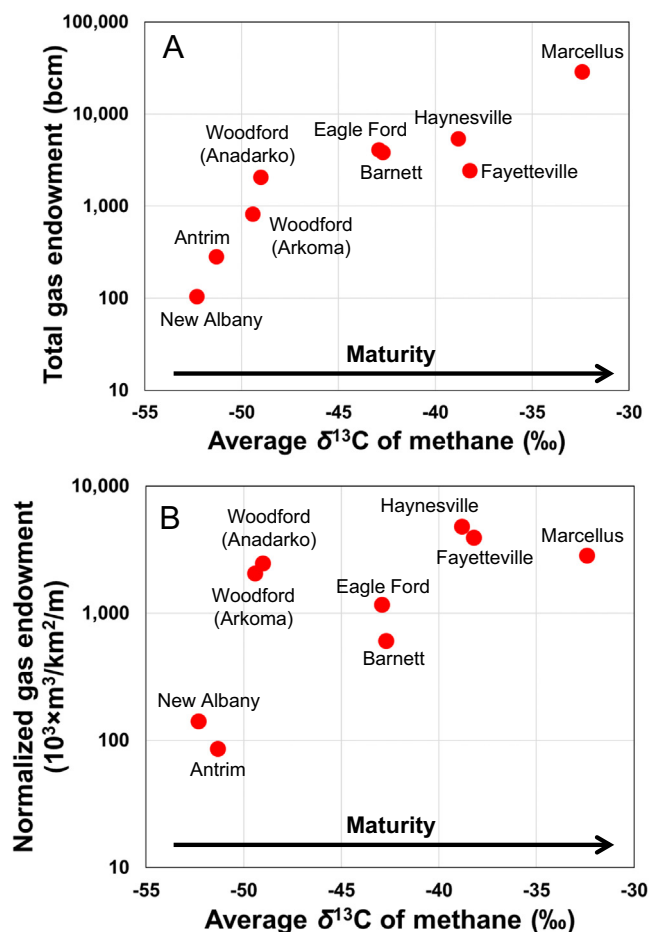
Fig. 19. Relationship between the average values of $\delta^{13}C$ of methane in produced gases from selected commercially successful plays and their total (A, in billion cubic meters) and normalized for area and thickness (B) gas endowments (the sum of produced gases (Energy Information Administration, 2019), reserves (Energy Information Administration, 2019) and technically recoverable resources (Potential Gas Agency, 2019)).

successful overseas plays such as Vaca Muerta (Argentina) and Wufeng-Longmaxi (China). Fig. 19A suggests that shale plays in the USA with more mature thermogenic gases have larger total gas endowments. Gas endowment depends on the area of the play, net thickness, porosity, gas saturation, amount of adsorbed gas, gas expansion factor, and gas recovery factor. Still, the larger gas endowment normalized for area and net thickness of the formation (data in Table 3) is typical for more thermally mature plays (Fig. 19B). Clearly, more mature shales generated and retained more volumes of natural gas. The implication from data in Fig. 19 is that most commercially successful shale plays should contain mid-mature (oil-associated) and late-mature mature thermogenic gases ($\delta^{13}C\text{-}C_1 > -50‰$), which can serve as a useful screening criteria in shale play evaluations. Still, we note that this conclusion is based only on a limited dataset from nine shale plays in the USA. Also, it is likely that the gas endowment of shale plays becomes smaller in very mature shale plays. Fig. 19B hints that the normalized gas endowment may start decreasing at $\delta^{13}C\text{-}C_1$ about $-35‰$ (as in the Marcellus Formation), and more data is necessary to test this hypothesis.

Shale gases with early-mature thermogenic origin and secondary microbial origin have been produced from naturally fractured shales in the New Albany Formation (Illinois Basin, USA) since 1858 (Nuttall, 2013) and from the Antrim Formation (Michigan Basin, USA) since at least 1980s (Dolton and Quinn, 1995;

Goodman and Maness, 2008). However, total gas production from these plays (Energy Information Administration, 2019) and their total gas endowment (Table 3) are much lower than in shale plays with mature thermogenic gases. This is, at least partially, because the process of secondary microbial gas generation and preservation from biodegraded petroleum fluids is less efficient than the process of thermogenic gas generation and preservation from kerogen and results in relatively lower gas content in shales.

To date, there are few examples of gas production from shale reservoirs containing primary microbial gases. Rice and Claypool (1981) reported production from shallow (328–647 m below surface) naturally fractured marl and chalk Niobrara Formation in Colorado and Kansas. The relatively dry gas ($C_1/(\sum C_1\text{-}C_5)$ between 0.976 and 0.999) and methane enriched in ^{12}C ($\delta^{13}C\text{-}C_1$ between -70.2 and $-54.7‰$) indicate various contributions of primary microbial, early-mature thermogenic and perhaps secondary microbial gases in these accumulations. However, these accumulations are not in the main commercial area of the Niobrara play where oil and associated thermogenic gas are produced via hydraulic fracturing in the deeper parts of the Denver Basin (Sonnenberg, 2013). It appears that the process of primary microbial gas generation is least efficient in formation and preservation of gases in shale reservoirs.

5. Conclusions

Gases from shale formations contain mostly methane and can have primary microbial, secondary microbial and thermogenic origins. It appears that most shale gases have thermogenic origin. This is especially true for gases from the most productive shale plays, both in the USA (e.g., Marcellus, Haynesville, Eagle Ford, Barnett) and overseas (e.g., Vaca Muerta in Argentina and Wufeng-Longmaxi in China). Shallower naturally fractured shales show evidence of oil biodegradation and secondary methanogenesis, due to infiltration of meteoric water from overlying aquifers. Plays with early mature thermogenic and secondary microbial gases (e.g., Antrim and New Albany in the USA) appear to be less productive than plays with mature thermogenic gases. There are few plays with primary microbial gases and they are, likely, not commercially viable due to low gas content. Reversed compound-specific carbon isotope trends are common in highly productive late-mature (VR > 2%) shales that experienced significant (>2 km) uplift. Although many processes can lead to isotope reversals and roll-overs in mature shale, we found that molecular and isotopic fractionation related to differential gas desorption during significant depressurization – first, from basin uplift and then from production – may be the leading mechanism in shale plays.

References

Abrams, M.A., Thomas, D., 2020. Geochemical evaluation of oil and gas samples from the Upper Devonian and Mississippian reservoirs Southern Anadarko

Basin Oklahoma and its implication for the Woodford Shale unconventional play. Marine and Petroleum Geology 112, 104043.

Bernard, B., Brooks, J.M., Sackett, W.M., 1976. Natural gas seepage in the Gulf of Mexico. Earth and Planetary Science Letters 31, 48–54.

Bernard, B., Brooks, J.M., Sackett, W.M., 1977. A geochemical model for characterization of hydrocarbon gas sources in marine sediments. In: 9th Annual OTC Conference, pp. 435–438 (OTC 2934).

Burruss, R.C., Laughrey, C.D., 2010. Carbon and hydrogen isotopic reversals in deep basin gas: evidence for limits to the stability of hydrocarbons. Organic Geochemistry 41, 1285–1296.

Byrne, D.J., Barry, P.H., Lawson, M., Ballentine, C.J., 2018a. Determining gas expulsion vs retention during hydrocarbon generation in the Eagle Ford Shale using noble gases. Geochimica et Cosmochimica Acta 241, 240–254.

Byrne, DJ., Barry, P.H., Lawson, M., Ballentine, C.J., 2018b. Noble gases in conventional and unconventional petroleum systems. Geological Society, London, Special Publications 468 (1), 127–149. https://doi.org/10.1144/SP468.5.

Byrne, D.J., Barry, P.H., Lawson, M., Ballentine, C.J., 2020. The use of noble gas isotopes to constrain subsurface fluid flow and hydrocarbon migration in the East Texas Basin. Geochimica et Cosmochimica Acta 268, 186–208.

Cander, H., 2012. Sweet spots in shale gas and liquids plays: Prediction of fluid composition and reservoir pressure. Search and Discovery Article #40936.

Cao, C., Tang, Q., Zhang, M., Lv, Z., 2015. Carbon isotope reversals of Changning-Weiyuan region shale gas, Sichuan basin. Acta Geologica Sinica (English Edition) 89 (supp), 375–377.

Cao, G., Zhang, H., Jiang, W., Wu, S., Zhu, D., Lin, M., 2019. A new gas-content-evaluation method for organic-rich shale using the fractionation of carbon isotopes of methane. SPE Journal. SPE 197043.

Chen, F., Jiang, C., Shi, P., Chen, J., Dong, J., Feng, D., Cheng, H., 2016. Geochemical characteristics of terrestrial shale gas and its production prediction significance in the Ordos Basin, China. Journal of Natural Gas Geoscience 1, 425–433.

Chung, H.M., Gormly, J.R., Squires, R.M., 1988. Origin of gaseous hydrocarbons in subsurface environments: theoretical considerations of carbon isotope distribution. Chemical Geology 71, 97–104.

Clog, M., Lawson, M., Peterson, B., Ferreira, A.A., Santos Neto, E.V., Eiler, J.M., 2018. A reconnaissance study of $^{13}C–^{13}C$ clumping in ethane from natural gas. Geochimica et Cosmochimica Acta 223, 229–244.

Coleman, D.D., 2001. -70‰ methane, is it biogenic or thermogenic? AAPG Search and Discovery Article #90906.

Curiale, J.A., Curtis, J.B., 2016. Organic geochemical applications to the exploration for source-rock reservoirs – a review. Journal of Unconventional Oil and Gas Resources 13, 1–31.

Curtis, J.B., 2002. Fractured shale-gas systems. American Association of Petroleum Geologists Bulletin 86, 1921–1938.

Dai, J., Xia, X., Qin, S., Zhao, J., 2004. Origins of partially reversed alkane $\delta^{13}C$ values for biogenic gases in China. Organic Geochemistry 35, 405–411.

Dai, J., Zou, C., Dong, D., Ni, Y., Wu, W., Gong, D., Wang, Y., Huang, S., Huang, J., Fang, C., Liu, D., 2016. Geochemical characteristics of marine and terrestrial shale gas in China. Marine and Petroleum Geology 76, 444–463.

Dai, J., Zou, C., Liao, S., Dong, D., Ni, Y., Huang, J., Wu, W., Gong, D., Huang, S., Hu, G., 2014. Geochemistry of the extremely high thermal maturity Longmaxi shale gas, southern Sichuan Basin. Organic Geochemistry 74, 3–12.

Dai, J.X., Zou, C.N., Zhang, S.C., Li, J., Ni, Y., Hu, G.Y., 2008. Discrimination of abiogenic and biogenic alkane gases. Science in China (Series D) 51, 1737–1749.

Darling, B.K., 2015. Origins of natural gas discharging from shallow groundwater. Journal of Petroleum Technology 67 (9), 20–21.

De Silva, P.N.K., Simons, S.J.R., Stevens, P., Philip, L.M., 2015. A comparison of North American shale plays with emerging non-marine shale plays in Australia. Marine and Petroleum Geology 67, 16–29.

Dolton, G.L., Quinn, J.C., 1995. An initial resource assessment of the Upper Devonian Antrim Shale in the Michigan basin. US Geological Survey Open-File Report 95-75K, 10 p.

Douglas, P.M.J., Stolper, D.A., Eiler, J.M., Sessions, A.L., Lawson, M., Shuai, Y., Bishop, A., Podlaha, O.G., Ferreira, A.A., Santos Neto, E.V., Niemann, M., Steen, A.S., Huang, L., Chimiak, L., Valentine, D.L., Fiebig, J., Luhmann, A.J., Seyfried, W.E., Etiope, G., Schoell, M., Inskeep, W.P., Moran, J.J., Kitchen, N., 2017. Methane clumped isotopes: progress and potential for a new isotopic tracer. Organic Geochemistry 113, 262–282.

East, J.A., Swezey, C.S., Repetski, J.E., Hayba, D.O., 2012. Thermal maturity map of Devonian shale in the Illinois, Michigan, and Appalachian basins of North America. US Geological Survey Scientific Investigations Map 3214, 1 sheet, scale 1:24,000.

Energy Information Administration, 2019, Natural gas sata, https://www.eia.gov/naturalgas/data.php#production (accessed on December 24, 2019).

Ellis, L., Berkman, T., Uchytil, S., Dzou, L., 2007. Integration of mud gas isotope logging (MGIL) with field appraisal at Horn Mountain Field, deepwater Gulf of Mexico. Journal of Petroleum Science and Engineering 58, 443–463.

Faiz, M., Altmann, C., Dunne, M., Baruch, E., Close, D., Cote, A., 2018a. Precambrian organic matter and thermal maturity of the Beetaloo Basin, Northern Territory, Australia. In: AESC – 2016 Australian Earth Sciences Convention, Uncover Earth's past to Discover Our Future, 26–30 June 2016, Adelaide Convention Centre. Geological Society of Australia, Hornsby, NSW, Australia, pp. 133.

Faiz, M., Zoitsas, A., Altmann, C., Baruch, E., Close, D., 2018b. Compositional variations and carbon isotope reversal in coal and shale gas reservoirs of the Bowen and Beetaloo basins, Australia. In: Dowey, P., Osborne, M., Volk, H. (Eds.), Application of Analytical Techniques to Petroleum Systems. Geological Society Special Publications, 484, 20 p.

Feng, Z., Huang, S., Wu, W., Xie, C., Peng, W., Cai, Y., 2017. Longmaxi shale gas geochemistry in Changning and Fuling gas fields, the Sichuan Basin. Energy Exploration & Exploitation 35, 259–278.

Formolo, M.J., Salacup, J.M., Petsch, S.T., Martini, A.M., Nüsslein, K., 2008. A new model linking atmospheric methane sources to Pleistocene glaciation via methanogenesis in sedimentary basins. Geology 36, 139–142.

Goodman, W.R., Maness, T.R., 2008. Michigan's Antrim gas shale play – a two-decade template for successful Devonian gas shale development. Search and Discovery Article #10158.

Gutsalo, L.K., Plotnikov, A.M., 1981. Carbon isotopic composition in the CH4-CO2 system as a criterion for the origin of methane and carbon dioxide in Earth natural gases (in Russian). Doklady Akademii Nauk SSSR 259, 470–473.

Györe, D., Pujol, M., Gilfillan, S., Stuart, F., Estrada, S., 2017. Using noble gas isotopes to constrain the source of CO2 in the Vaca Muerta Shale in the Neuquén Basin (Argentina). Goldschmidt 2017, Abstract.

Hao, F., Guo, T., Zhu, Y., Cai, X., Zou, H., Li, P., 2008. Evidence for multiple stages of oil cracking and thermochemical sulfate reduction in the Puguang gas field, Sichuan Basin, China. American Association of Petroleum Geologists Bulletin 92, 611–637.

He, D., 2017. Thermal Maturity, Composition and Origin of the Hydrocarbon Gases of the Eagle Ford shale in Texas, USA Senior Thesis. Ohio State University, p. 25.

Hill, D.G., Nelson, C.R., 2000. Gas productive fractured shales: an overview and update. GasTIPS 6, 4–13.

Hoffmann, T.W., 2016. Roper Basin burial history modelling: inferences for the timing of hydrocarbon generation. In: Annual Geoscience Exploration Seminar (AEGS) Proceedings, Alice Springs, Northern Territory 15–16 March 2016. Northern Territory Geological Survey, Darwin, Australia, pp. 100–107.

Howarth, R.W., 2019. Ideas and perspectives: is shale gas a major driver of recent increase in global atmospheric methane? Biogeosciences 16, 3033–3046. https://doi.org/10.5194/bg-16-3033-2019.

James, A.T., Burns, B.J., 1984. Microbial alteration of subsurface natural gas accumulations. American Association of Petroleum Geologists Bulletin 68, 957–960.

Jarvie, D., 2004. Evaluation of hydrocarbon generation and storage in the Barnett shale, Ft. Worth Basin, Texas. Special BEG/PTTC Presentation. http://teamfrack.pbworks.com/w/file/fetch/48478518/Evaluation%20of%20Hydrocarbon%20Genration%20and%20Storage%20in%20the%20Barnett%20Shale.pdf (accessed on January 15, 2020).

Jenden, P., Drazan, D., Kaplan, I., 1993. Mixing of thermogenic natural gases in northern Appalachian Basin. American Association of Petroleum Geologists Bulletin 77, 980–998.

Kornacki, A.S., Dahl, J.E., 2016. Evidence some oil accumulations in the Woodford formation and the Meramec formation received an additional charge of very dry thermal gas. Search and Discovery Article #41879.

Krasnova, E.A., Yurchenko, A.Yu, Kalmykov, A.G., Fomina, M.M., 2019. Isotopic-geochemical peculiarities of the distribution of gas hydrocarbons in the Bazhenov formation section (South part of the Western Siberia). Georesources 21, 153–158. https://doi.org/10.18599/grs.2019.2.153-158 (in Russian).

Krouse, H.R., Viau, C.A., Eliuk, L.S., Ueda, A., Halas, S., 1988. Chemical and isotopic evidence of thermochemical sulphate reduction by light hydrocarbon gases in deep carbonate reservoirs. Nature 333, 415–419.

Lamb, J., 2014. An Examination of the Arkoma Foreland Basin and its Petroleum System Through Burial and Thermal History Modeling MSc thesis. University of Houston, p. 160.

Laughrey, C.D., 2014. Geochemical characterization of post-mature gases from Middle Devonian Marcellus Formation, Northern Appalachian Basin, USA – Insights into deep basin hydrocarbon generation, alteration, and productivity. AAPG 2014 Annual Convention and Exhibition, Houston, Texas, April 6–9, 2014. Search and Discovery Article #80384.

Lewan, M., 1997. Experiments on the role of water in petroleum formation. Geochimica et Cosmochimica Acta 61, 3691–3723.

Lillis, P.G., Warden, A., Claypool, G.E., Magoon, L.B., 2007. Petroleum systems of the San Joaquin Basin Province – geochemical characteristics of gas types. In: Petroleum Systems and Geologic Assessment of Oil and Gas in the San Joaquin Basin Province, California. USGS Prof Paper 1713, pp. 1–30.

Li, J., Zhou, S., Fu, D., Chen, K., Zhang, C., Sun, Z., Li, P., 2019. Characteristics of desorption gas of lacustrine shale in the Ordos Basin, China. IOP Conference Series, Earth and Environmental Science 360. https://doi.org/10.1088/1755-1315/360/1/012020.

Li, S., Yuan, Y., Sun, W., Sun, D., Jin, Z., 2016. Formation and destruction mechanism as well as major controlling factors of the Silurian shale gas overpressure in the Sichuan Basin, China. Journal of Natural Gas Geoscience 1, 287–294.

Liu, C., Liu, P., McGovern, G.P., Horita, J., 2019a. Molecular and intramolecular isotope geochemistry of natural gases from the Woodford Shale, Arkoma Basin, Oklahoma. Geochimica et Cosmochimica Acta 255, 188–204.

Liu, Y., Zhang, J., Ren, J., Liu, Z., Huang, H., Tang, X., 2016a. Stable isotope geochemistry of the nitrogen-rich gas from lower Cambrian shale in the Yangtze Gorges area, South China. Marine and Petroleum Geology 77, 693–702.

Liu, Y., Zhang, J., Tang, X., 2016b. Predicting the proportion of free and adsorbed gas by isotopic geochemical data: a case study from lower Permian shale in the southern North China basin (SNCB). International Journal of Coal Geology 156, 25–35.

Liu, Y., Tang, X., Zhang, J., Mo, X., Huang, H., Liu, Z., 2018. Geochemical characteristics of the extremely high thermal maturity transitional shale gas in the Southern North China Basin (SNCB) and its differences with marine shale gas. International Journal of Coal Geology 194, 33–44.

Liu, Z., Chen, D., Zhang, J., lv, X., Dang, W., Liu, Y., Liao, W., Li, J., Wang, Z., Wang, F., 2019b. Combining isotopic geochemical data and logging data to predict the range of the total gas content in shale: a case study from the Wufeng and Longmaxi shales in the middle Yangtze area, South China. Energy Fuels 33, 10487–10498.

Ma, Y., Zhong, N., Yao, L., Huang, H., Larter, S., Jiao, W., 2020. Shale gas desorption behavior and carbon isotopic variations of gases from canister desorption of two sets of gas shales in south China. Marine and Petroleum Geology 113. https://doi.org/10.1016/j.marpetgeo.2019.104127.

Martini, A.M., Walter, L.M., Ku, T.C.W., Budai, J.M., McIntosh, J.C., Schoell, M., 2003. Microbial production and modification of gases in sedimentary basins: a geochemical case study from a Devonian shale gas play, Michigan basin. American Association of Petroleum Geologists Bulletin 87, 1355–1375.

Mastalerz, M., Drobniak, A., Schimmelmann, A., 2017. Characteristics of microbial coalbed gas during production; example from Pennsylvanian coals in Indiana, USA. Geosciences 7, 26.

McIntosh, J.C., Walter, L.M., Martini, A.M., 2002. Pleistocene recharge to midcontinent basins: effects on salinity structure and microbial gas generation. Geochimica et Cosmochimica Acta 66, 1681–1700.

Meng, Q., Wang, X., Wang, X., Shi, B., Luo, X., Zhang, L., Lei, Y., Jiang, C., Liu, P., 2017. Gas geochemical evidences for biodegradation of shale gases in the Upper Triassic Yanchang Formation, Ordos Basin, China. International Journal of Coal Geology 179, 139–152.

Milkov, A.V., 2010. Methanogenic biodegradation of petroleum in the West Siberian basin (Russia): significance for formation of giant Cenomanian gas pools. American Association of Petroleum Geologists Bulletin 94, 1485–1541.

Milkov, A.V., 2011. Worldwide distribution and significance of secondary microbial methane formed during petroleum biodegradation in conventional reservoirs. Organic Geochemistry 42, 184–207.

Milkov, A.V., 2018. Secondary microbial gas. In: Wilkes, H. (Ed.), Hydrocarbons, Oils and Lipids: Diversity, Origin, Chemistry and Fate. Handbook of Hydrocarbon and Lipid Microbiology. Springer, Cham.

Milkov, A.V., Etiope, G., 2018. Revised genetic diagrams for natural gases based on a global dataset of >20,000 samples. Organic Geochemistry 125, 109–120.

Milkov, A.V., Claypool, G.E., Lee, Y.-J., Torres, M.E., Borowski, W.S., Tomaru, H., Sassen, R., Long, P.E., ODP Leg 204 Scientific Party, 2004. Ethane enrichment and propane depletion in subsurface gases indicate gas hydrate occurrence in marine sediments at southern Hydrate Ridge offshore Oregon. Organic Geochemistry 35, 1067–1080.

Milkov, A.V., Goebel, E., Dzou, L., Fisher, D.A., Kutch, A., McCaslin, N., Bergman, D.F., 2007. Compartmentalization and time-lapse geochemical reservoir surveillance of the Horn Mountain oil field, deep-water Gulf of Mexico. American Association of Petroleum Geologists Bulletin 91, 847–876.

Milkov, A.V., Schwietzke, S., Allen, G., Sherwood, O.A., Etiope, G., 2020. Using global isotopic data to constrain the role of shale gas production in recent increases in atmospheric methane, Scientific Reports 10, 4199 (2020), https://doi.org/10.1038/s41598-020-61035-w.

Molofsky, L.F., Connor, J.A., Wylie, A.S., Wagner, T., Farhat, S.K., 2013. Evaluation of methane sources in groundwater in Northeastern Pennsylvania. Groundwater 51, 333–349.

Nicot, J.-P., Larson, T., Darvari, R., Mickler, P., Slotten, M., Aldridge, J., Uhlman, K., Costley, R., 2017. Controls on methane occurrences in shallow aquifers overlying the Haynesville shale gas field, East Texas. Groundwater 55, 443–454. https://doi.org/10.1111/gwat.12500.

Niemann, M., Whiticar, M.J., 2017. Stable isotope systematics of coalbed gas during desorption and production. Geosciences 7, 43.

Norville, G., Muehlenbachs, K., 2018. Insights from stable isotope geochemistry surveillance in the unconventional Horn River Basin play. In: Unconventional Resources Technology Conference (URTeC), Houston, Texas, USA, 23–25 July 2018, https://doi.org/10.15530/urtec-2018-2901086.

Nunn, J.A., 2012. Burial and thermal history of the Haynesville shale: implications for overpressure, gas generation, and natural hydrofracture. GCAGS Journal 1, 81–96.

Nuttall, B.C., 2013. Middle and Late Devonian New Albany shale in the Kentucky Geological Survey Marvin Blan No. 1 well, Hancock County, Kentucky. Report of Investigations 17, Series XII, Kentucky Geological Survey, 72 p.

Nuttall, B.C., Parris, T.M., Beck, G., Willette, D.C., Mastalerz, M., Crockett, J., 2015. Oil production from low-maturity organic-rich shale: An example from the Devonian New Albany shale in the Illinois Basin, Breckinridge county, Kentucky. Search and Discovery Article #51196.

Osborn, S.G., McIntosh, J.C., 2010. Chemical and isotopic tracers of the contribution of microbial gas in Devonian organic-rich shales and reservoir sandstones, northern Appalachian Basin. Applied Geochemistry 25, 456–471.

Pan, C., Yu, L., Liu, J., Fu, J., 2006. Chemical and carbon isotopic fractionations of gaseous hydrocarbons during abiogenic oxidation. Earth and Planetary Science Letters 246, 70–89.

Peebles, M.W.H., 1980. Evolution of the Gas Industry. New York University Press, New York, p. 235.

Petersen, H.I., Hillock, P., Milner, S., Pendlebury, M., Scarlett, D., 2019. Monitoring gas distribution and origin in the Culzean field, UK Central North Sea, using data from a continuous isotope logging tool and Isotube and test samples. Journal of Petroleum Geology 42, 435–450.

Piasecki, A., Sessions, A., Lawson, M., Ferreira, A.A., Santos Neto, E.V., Ellis, G.S., Lewan, M.D., Eiler, J.M., 2018. Position-specific ^{13}C distributions within propane from experiments and natural gas samples. Geochimica et Cosmochimica Acta 220, 110–124.

Potential Gas Agency (2019) Potential supply of natural gas in the United States: Report of the Potential Gas Committee (December 31, 2018). Colorado School of Mines, 106 p.

Potter, C.J., 2018. Paleozoic shale gas resources in the Sichuan Basin, China. American Association of Petroleum Geologists Bulletin 102, 987–1009.

Price, L.C., 2001. A possible deep-basin-high-rank gas machine via water-organic-matter redox reactions. US Geological Survey. Digital Data Series, p. 67 (Chapter H).

Prinzhofer, A., Girard, J.P., Buschaert, S., Huiban, Y., Noirez, S., 2009. Chemical and isotopic characterization of hydrocarbon gas traces in porewater of very low permeability rocks: the example of the Callovo-Oxfordian argillites of the eastern part of the Paris Basin. Chemical Geology 260, 269–277.

Qin, H., Fan, X., Liu, M., Hao, J., Liang, B., 2017. Carbon isotope reversal of desorbed gas in Longmaxi shale of Jiaoshiba area, Sicuhan Basin. Petroleum Research 2, 169–177.

Reese, S.O., Neboga, V.V., Pelepko, S., Kosmer, W.J., Beattie, S., 2014. Groundwater and petroleum resources of Sullivan County, Pennsylvania. Pennsylvania Geological Survey, Fourth Series, Water Resource Report 71, 99 p.

Rice, D.D., Claypool, G.E., 1981. Generation, accumulation, and resource potential of biogenic gas. American Association of Petroleum Geologists Bulletin 61, 5–25.

Rodriguez, N.D., Philp, R.P., 2010. Geochemical characterization of gases from the Mississippian Barnett Shale, Fort Worth Basin, Texas. American Association of Petroleum Geologists Bulletin 94, 1641–1656.

Roen, J.B., 1993. Introductory review – Devonian and Mississippian black shale, eastern North America. In: Roen, J.B., Kepferle, R.C. (Eds.), Petroleum geology of the Devonian and Mississippian black shale of eastern North America. US Geological Survey Bulletin 1909, p. A1–A8.

Rowan, E.L., 2006. Burial and thermal history of the Central Appalachian basin, based on three 2-D models of Ohio, Pennsylvania, and West Virginia. US Geological Survey Open-File Report 2006-1019, 35 p.

Rowe, D., Muehlenbachs, K., 1999a. Isotopic fingerprints of shallow gases in the Western Canadian sedimentary basin: tools for remediation of leaking heavy oil wells. Organic Geochemistry 30, 861–871.

Rowe, D., Muehlenbachs, K., 1999b. Low-temperature thermal generation of hydrocarbon gases in shallow shales. Nature 398, 61–63.

Saadati, H., Al-Iessa, H.J., Alizadeh, B., Tarhandeh, E., Jazayeri, M.H., Bahrami, H., Rashidi, M., 2016. Geochemical characteristics and isotopic reversal of natural gases in eastern Kopeh-Dagh, NE Iran. Marine and Petroleum Geology 78, 76–87.

Salehi, I., 2010. New Albany shale gas project 07122-16. RPSEA Final Report, 102 p.

Sassen, R., Sweet, S.T., DeFreitas, D.A., Milkov, A.V., 2000. Exclusion of 2-methylbutane (isopentane) during crystallization of structure II gas hydrate in sea-floor sediment, Gulf of Mexico. Organic Geochemistry 31, 1257–1262.

Schlegel, M.E., McIntosh, J.C., Bates, B.L., Kirk, M.F., Martini, A.M., 2011. Comparison of fluid geochemistry and microbiology of multiple organic-rich reservoirs in the Illinois Basin, USA: evidence for controls on methanogenesis and microbial transport. Geochimica et Cosmochimica Acta 75, 1903–1919.

Schoell, M., 1983. Genetic characterization of natural gases. American Association of Petroleum Geologists Bulletin 67, 2225–2238.

Schovsbo, N.H., Nielsen, A.T., 2017. Generation and origin of natural gas in Lower Palaeozoic shales from southern Sweden. Geological Survey of Denmark and Greenland Bulletin 38, 37–40.

Schulz, H.-M., Biermann, S., van Berk, W., Krüger, M., Straaten, N., Bechtel, A., Wirth, R., Lüders, V., Schovsbo, N.H., Crabtree, S., 2015. From shale oil to biogenic shale gas: retracing organic–inorganic interactions in the Alum Shale (Furongian–Lower Ordovician) in southern Sweden. American Association of Petroleum Geologists Bulletin 99, 927–956.

Schwietzke, S., Sherwood, O.A., Bruhwiler, L.M.P., Miller, J.B., Etiope, G., Dlugokencky, E.J., Englund Michel, S., Arling, V.A., Vaughn, B.H., White, J.W.C., Tans, P.P., 2016. Upward revision of global fossil fuel methane emissions based on isotope database. Nature 538, 88–91.

Sharma, S., Bowman, L., Schroeder, K., Hammack, R., 2015. Assessing changes in gas migration pathways at a hydraulic fracturing site: example from Greene County, Pennsylvania, USA. Applied Geochemistry 60, 51–58.

Sherwood Lollar, B., Westgate, T.D., Ward, J.A., Slater, G.F., Lacrampe-Couloume, G., 2002. Abiogenic formation of alkanes in the Earth's crust as a minor source for global hydrocarbon reservoirs. Nature 416, 522–524.

Shuai, Y., Etiope, G., Zhang, S., Douglas, P.M.J., Huang, L., Eiler, J.M., 2018. Methane clumped isotopes in the Songliao Basin (China): new insights into abiotic vs. biotic hydrocarbon formation. Earth and Planetary Science Letters 482, 213–221.

Sonnenberg, S.A., 2013. New reserves in an old field, the Niobrara resource play in the Wattenberg Field, Denver Basin, Colorado. Unconventional Resources Technology Conference, Denver, Colorado, USA, 12–14 August 2013, URTeC 1562913.

Stolper, D.A., Lawson, M., Davis, C.L., Ferreira, A.A., Santos Neto, E.V., Ellis, G.S., Lewan, M.D., Martini, A.M., Tang, Y., Schoell, M., Sessions, A.L., Eiler, J.M., 2014. Formation temperatures of thermogenic and biogenic methane. Science 344, 1500–1503.

Strąpoć, D., Mastalerz, M., Schimmelmann, A., Drobniak, A., Hasenmueller, N.R., 2010. Geochemical constraints on the origin and volume of gas in the New Albany Shale (Devonian–Mississippian), eastern Illinois Basin. American Association of Petroleum Geologists Bulletin 94, 1713–1740.

Sun, Z., Wang, Y., Wei, Z., Zhang, M., Wang, G., Wang, Z., 2017. Characteristics and origin of desorption gas of the Permian Shanxi Formation shale in the Ordos Basin, China. Energy Exploration & Exploitation 35, 792–806.

Tang, Y., Xia, D., 2011. Quantitative assessment of shale-gas potential based on its special generation and accumulation processes: Search and Discovery Article #40819, http://www.searchanddiscovery.com/pdfz/documents/2011/40819tang/ndx_tang.pdf.html (website accessed September 5, 2019).

Telling, J., Lacrampe-Couloume, G., Sherwood Lollar, B., 2013. Carbon and hydrogen isotopic composition of methane and C_{2+} alkanes in electrical spark discharge: implication for identifying sources of hydrocarbons in terrestrial and extraterrestrial settings. Astrobiology 13, 483–490.

Tilley, B., Muehlenbachs, K., 2013. Isotope reversals and universal stages and trends of gas maturation in sealed, self-contained petroleum systems. Chemical Geology 339, 194–204.

Tilley, B., McLellan, S., Hiebert, S., Quartero, B., Veilleux, B., Muehlenbachs, K., 2011. Gas isotope reversals in fractured gas reservoirs of the western Canadian Foothills: mature shale gases in disguise. American Association of Petroleum Geologists Bulletin 95, 1399–1422.

Ulmishek, G.F., 2003. Petroleum geology and resources of the West Siberian Basin, Russia. US Geological Survey Bulletin 2201-G, 49.

Vinogradov, A.P., Galimov, E.M., 1970. Isotopism of carbon and the problem of oil origin. Geochemistry 3, 275–297.

Wang, X., Jiang, Z., Zhang, K., Wen, M., Xue, Z., Wu, W., Huang, Y., Wang, Q., Liu, X., Liu, T., Xie, X., 2020. Analysis of gas composition and nitrogen sources of shale gas reservoir under strong tectonic events: evidence from the complex tectonic area in the Yangtze Plate. Energies 13, 281. https://doi.org/10.3390/en13010281.

Wei, X., Guo, T., Liu, R., 2016. Geochemical features and genesis of shale gas in the Jiaoshiba block of Fuling Shale gas field, Chongqing, China. Journal of Natural Gas Geoscience 1, 361–371.

Wen, T., Castro, M.C., Ellis, B.R., Hall, C.M., Lohmann, K.C., 2015. Assessing compositional variability and migration of natural gas in the Antrim Shale in the Michigan Basin using noble gas geochemistry. Chemical Geology 417, 356–370.

Williams, K.E., 2013. Burial history modeling and paleogeomechanics of the Barnett and Haynesville. Search and Discovery Article #50807.

Whiticar, M.J., Faber, E., Schoell, M., 1986. Biogenic methane formation in marine and freshwater environments: CO_2 reduction vs. acetate fermentation – isotope evidence. Geochimica et Cosmochimica Acta 50, 693–709.

Xia, X., Chen, J., Braun, R., Tang, Y., 2013. Isotopic reversals with respect to maturity trends due to mixing of primary and secondary products in source rocks. Chemical Geology 339, 205–212.

Xia, X., Tang, Y., 2012. Isotope fractionation of methane during natural gas flow with coupled diffusion and adsorption/desorption. Geochimica et Cosmochimica Acta 77, 489–503.

Yang, R., He, S., Hu, Q., Hu, D., Yi, J., 2017. Geochemical characteristics and origin of natural gas from Wufeng-Longmaxi shales of the Fuling gas field, Sichuan Basin (China). International Journal of Coal Geology 171, 1–11.

Zhang, M., Tang, Q., Cao, C., Lv, Z., Zhang, T., Zhang, D., Li, Z., Du, L., 2018. Molecular and carbon isotopic variation in 3.5 years shale gas production from Longmaxi Formation in Sichuan Basin, China. Marine and Petroleum Geology 89, 27–37.

Zhang, T., Ellis, G.S., Ruppel, S.C., Milliken, K., Yang, R., 2012. Effect of organic-matter type and thermal maturity on methane adsorption in shale-gas systems. Organic Geochemistry 47, 120–131.

Zhao, H., Liu, W., Wang, X., 2018. The openness degree study of the Jiaoshiba shale gas, Sichuan Basin, China – potential factor responsible for reversed isotope series. Acta Geologica Sinica (English edition) 92, 2457–2459.

Zumberge, J., Ferworn, K., Brown, S., 2012. Isotopic reversal ('rollover') in shale gases produced from the Mississippian Barnett and Fayetteville formations. Marine and Petroleum Geology 31, 43–52.

Zumberge, J.E., Curtis, J.B., Reed, J.D., Brown, S.W., 2016. Migration happens: geochemical evidence for movement of hydrocarbons in unconventional petroleum systems. In: Unconventional Resources Technology Conference, San Antonio, Texas, USA, 1–3 August 2016, URTeC 2461914.